Trees and flowers on a billiard table

Olga Paris-Romaskevich

TREES AND FLOWERS ON A BILLIARD TABLE

by

Olga Paris-Romaskevich

to Manya and Katya

Abstract. — In this work we study the dynamics of triangle tiling billiards. We unite geometric and combinatorial approaches in order to prove several conjectures. In particular, we prove the Tree Conjecture and the $4n+2$ Conjecture, both stated by Baird-Smith, Davis, Fromm and Iyer. Moreover, we study the set of exceptional trajectories which is closely related to the set of minimal Arnoux-Rauzy maps and prove that all of such trajectories pass by all tiles. Finally, we prove that the arithmetic orbits of the Arnoux-Yoccoz map converge, up to rescaling, to the Rauzy fractal, as conjectured by Hooper and Weiss.

***Résumé* (Arbres et fleurs sur une table de billard).** — Nous étudions ici la dynamique des billards dans les pavages triangulaires périodiques. Nous réunissons des approches géométrique et combinatoire pour prouver quelques conjectures. En particulier, nous prouvons la Conjecture d'arbre et la Conjecture $4n+2$ formulés par Baird-Smith, Davis, Fromm et Iyer. Puis, nous étudions l'ensemble des trajectoires exceptionelles qui est lié à l'ensemble des applications minimales d'Arnoux-Rauzy, et nous prouvons que ces trajectoires passent par toute tuile. Finalement, nous prouvons que les orbites arithmetiques de l'application d'Arnoux-Yoccoz convergent à la fractale de Rauzy, modulo changement d'échelle, comme c'était conjecturé par Hooper et Weiss.

INTRODUCTION, MOTIVATION AND OVERVIEW OF RESULTS

A tiling billiard is a model of light propagation in a heterogeneous medium constructed as a union of homogeneous pieces, see [**18**] and [**20**]. For any tiling of a plane by polygons, a **tiling billiard** billiard on it is defined as follows. A light ray moves in a straight line till a moment when it reaches a border of a tile. Then it passes to the neighboring tile, and its direction follows Snell's law with a refraction coefficient $k \equiv -1$, see Figure 1. The dynamics of a tiling billiard depends very strongly on the shapes (but not sizes) of tiles in the underlying tiling.

The study of tiling billiards has been proposed in [**18**] and continued in [**12, 16, 25**]. For now, only two non-trivial examples of tiling billiards have been undestood, a trihexagonal tiling (see [**16**]) and a periodic triangle tiling (see [**12, 25**] and this work). Tiling billiards are of interest because of their relation to the study orientable vertical foliations on non-orientable flat surfaces, a non-explored area of the general theory.

The materials with the refraction index equal to -1 can be quite easily constructed (as slabs of photonic crystals) even though most of usual materials have refraction indices bigger than 1. An even more physically relevant tiling billiard model should incorporate a refraction coefficient $k(f)$ as a function of light frequency f. The tiling billiards dynamics corresponds to the resonances in the full wave picture. The research in physics and optics of metamaterials is very active, see in particular [**21, 30, 22, 36**], with numerous applications such as invisibility, see [**41**].

This work considers tiling billiards on two tilings with many common features. These are a **triangle tiling** and a **cyclic quadrilateral tiling** and are defined by applying central symmetries to a fixed triangular (or cyclic, i.e. inscribed in a circle, quadrilateral) shape with respect to the middle points of its edges, see Figure 2.

2000 ***Mathematics Subject Classification.*** — 37E05, 37E15, 37E20, 37N20.
Key words and phrases. — tiling billiards, Arnoux-Rauzy maps, Rauzy fractal.

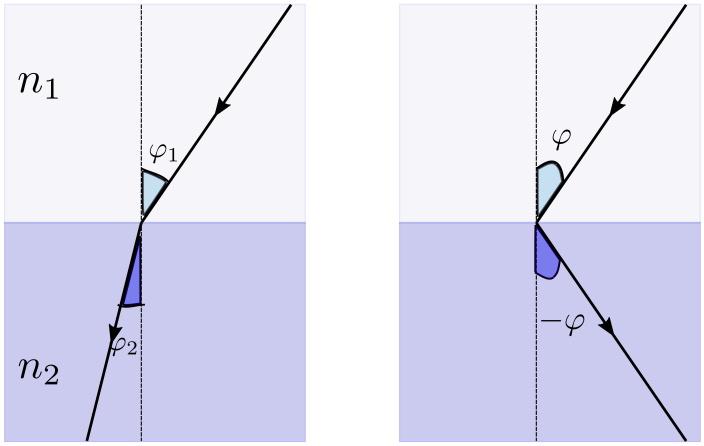

FIGURE 1. *Snell's law of refraction.* On the left: a ray of light crosses the boundary between two media with refraction indices $n_1, n_2 \in \mathbf{R}$ and refracts. The relationship between the angles φ_1 and φ_2 is defined by $\frac{\sin\varphi_1}{\sin\varphi_2} = \frac{n_2}{n_1} =: k$. For example, for the passage from air ($n_1 \approx 1$) to water ($n_2 \approx 1.333$), $k \approx 0.75$. On the right: the behavior of a ray of light when $k = -1$.

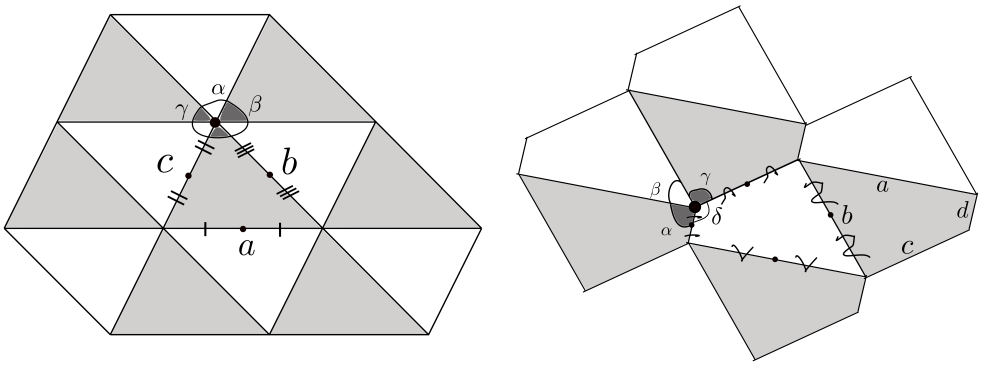

FIGURE 2. *A triangle and cyclic quadrilateral tilings.* For each vertex a sum of adjacent tile angles of a fixed color is equal to π. For the triangle tiling such a relation is trivial, and for a quadrilateral tiling it is equivalent to cyclicity.

We denote the angles of a tile by α, β, γ (and δ) and the sides by a, b and c (and d). We suppose that any tile is oriented so that a counterclockwise tour of its boundary reads the sides in the alphabetical order. Both tilings are 2-colorable. We call the tiles of one of the colors **positively oriented**, and of another color **negatively oriented**, in an arbitrary way.

Triangle tiling billiards were studied in **[18]** and in **[25]**. Even though some understanding of the dynamics has been achieved, a precise description of symbolic dynamics was far from being complete. Triangle tiling billiards are especially attractive because of their relation to the classical Arnoux-Rauzy family of IETs on the circle and the real-rel deformations of corresponding translation surfaces. In the present work we give a complete description of the dynamics.

1. Symbolic dynamics of triangle tiling billiards

1.1. Overview of known results. — Let $\mathcal{A}_\Delta := \{a, b, c\}$. A **symbolic code** of an oriented curve on the tiled plane is a word in $\mathcal{A}_\Delta^{\mathbf{N}}$ that corresponds to the sequence of sides of triangular tiles, crossed by it. We denote by $\overline{w}$ an infinite periodic word with period w. An **accelerated symbolic code** in the alphabet $\mathcal{A}_\Delta^2 := \{ab, ba, bc, cb, ca, ac\}$ is defined analogously as a sequence of couples of croissed edges. For example, a symbolic (or an accelerated symbolic) code of a curve making a clockwise tour of a vertex is equal to $\overline{abc}$ (or $\overline{ab\ bc\ ca}$). This defines the **symbolic dynamics of triangle tiling billiards** via the shift map on the space of admissible sequences.

Example. — A symbolic code of a periodic trajectory from Figure 3 is given by a periodic word $\overline{w}$ with minimal period $w = abacacacbacac$ (half of the trajectory).

The state of art on the symbolic behavior of trajectories is summarized in

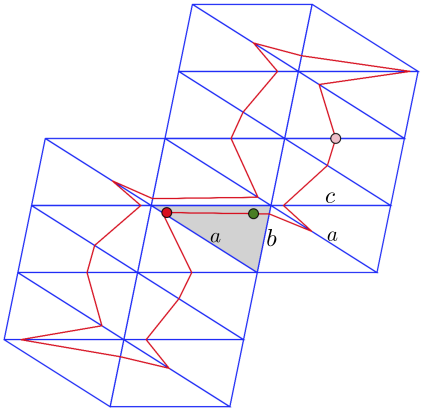

FIGURE 3. *A periodic trajectory and the labelling of the edges along it.*

Theorem 1. — **[12, 25]** *Consider a triangle tiling billiard. Then the following holds:*

1. *Every trajectory passes by each tile at most once; the oriented distance between a segment of a trajectory in a tile and its circumcenter is an invariant of the trajectory;*
2. *all bounded trajectories are periodic and simple closed curves;*
3. *all bounded trajectories deform to the trajectories with the same symbolic code under small perturbations (form of a tile, initial condition);*
4.* *the period of any periodic trajectory belongs to the set* $\{4n+2 \mid n \in \mathbf{N}^*\}$*;*
5.* *the symbolic code of any periodic trajectory has its smallest period* $w \in \mathcal{A}_\Delta$ *of odd length.*

This theorem implies tha the periodicity is an open property and trajectory on Figure 3 is stable. The points 1.–3. have been proven and 4. has been conjectured in **[12]**. The points 1.–3. follow from the *folding*, see Section 3. The point 4. is a simple consequence of 5. The statements 4.–5. have been announced to be proven in **[25]** by P. Hubert and myself. Our proof is based on the relation (see **[12]**) of triangle tiling billiards with interval exchange transformations (IETs) with flips, is quite technical and, unfortunately, incomplete as we have discovered while working on this paper, see more comments in the Appendix. In this work, we give a first complete proof of 4. and 5., known as $4n+2$ Conjecture, see **[12]**.

We say that a triangle tiling billiard trajectory is **escaping** if it is not periodic. This definition makes sense by point 1. of the theorem above. A trajectory is **linearly escaping** if it escapes to infinity by staying in a bounded distance from a fixed line. Any triangle tiling billiard trajectory is either **periodic**, **linearly escaping** or **non-linearly escaping**, as follows from 1.–2. in Theorem 1, **[12]**. Moreover, any trajectory of a tiling billiard in *almost any* fixed triangle tiling *is either periodic or linearly escaping*, **[25]**. We now define a set of measure 0 if triangle tilings on which the trajectories can potentially non-linearly escape.

Let $\Delta_2 := \{(x_1, x_2, x_3) | x_i \geq 0, x_1 + x_2 + x_3 = 1\} \subset \mathbf{R}^3$ and define the **Rauzy subtractive algorithm** on Δ_2 as follows. If $x_j > \frac{1}{2}$ for some j, one maps a triple (x_1, x_2, x_3) to a new triple (x_1', x_2', x_3'), where $x_j' := 2x_j - 1$ and $x_i' = x_i, i \neq j$. Then we normalize by x_j to get back to Δ_2. In projective coordinates, this is equivalent to subtracting the sum of two smaller coordinates from the biggest one. The subset $\overline{\mathcal{R}} \subset \Delta_2$ of triples on which the Rauzy subtractive algorithm can be applied infinitely, was first defined in **[7]** by P. Arnoux and S. Starosta. They have proven that it is homeomorphic to the Sierpinsky triangle. We define $\mathcal{R} \subset \overline{\mathcal{R}}$ for which $x_j \neq \frac{1}{2}$ at each step of the Rauzy subtractive algorithm. In the following we call this set $\mathcal{R}$ the **Rauzy gasket**. The set $\mathcal{R}$ appears as a set of parameters of *interesting* maps in various dynamical contexts and is of great interest, see for example the works by Avila-Hubert-Skripchenko on systems of isometries **[10, 11]**, by Dynnikov-DeLeo **[19]** on sections of 3-periodic surfaces, by Arnoux-Rauzy **[6]** on 6−IETs on the circle. This set is also related to the dynamics of tiling billiards since it parametrizes the triangle tilings admitting non-linearly escaping trajectories. It is an open question to calculate $\dim_H \mathcal{R}$.

Consider the set of triangular tiles such that the point $\rho_\Delta \in \Delta_2$ defined by

$$\rho_\Delta := \left(1 - \frac{2}{\pi}\alpha, 1 - \frac{2}{\pi}\beta, 1 - \frac{2}{\pi}\gamma\right) \tag{1}$$

verifiers $\rho_\Delta \in \mathcal{R}$. A trajectory of a triangle tiling billiard is **exceptional** if it passes through the circumcenter of its starting tile (and hence, any crossed tile) and $\rho_\Delta \in \mathcal{R}$. Exceptional trajectories of triangle tiling billiards are of great interest since they describe the arithmetic orbits of minimal maps in the Arnoux-Rauzy family.

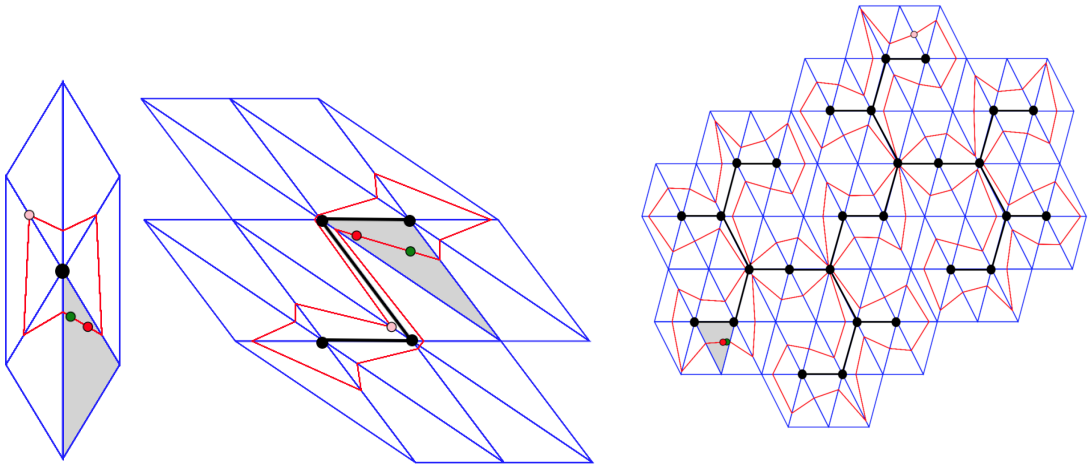

FIGURE 4. *Billiard trajectories and corresponding trees.*

Theorem 2. — **[25]** *Fix a triangle tiling. If $\rho_\Delta \notin \mathcal{R}$ then all of the trajectories in such a tiling are either periodic or linearly escaping. On the contrary, if $\rho_\Delta \in \mathcal{R}$, a trajectory escapes to infinity non-linearly* only if *it passes by the circumcenters of tiles.*

In the second part of this work, we prove that the *only if* can be replaced by *if and only if*. It has already been proven in **[25]** for almost all $\rho_\Delta \in \mathcal{R}$ with respect to the Avila-Hubert-Skripchenko measure on the Rauzy gasket defined in **[10, 11]**.

1.2. Tree Conjecture: formulation and motivation. — Consider a triangle tiling. Denote by $\Lambda_\Delta := (V, E)$ an abstract graph (with its natural embedding in the tiled plane) such that the set V consists of the vertices of tiles in the plane, two vertices in V being connected by an edge in E if they are connected in the tiling. For any periodic billiard trajectory δ we denote a **domain** of the plane **that it encloses** by $\Omega^\delta \subset \mathbf{R}^2$, $\partial\Omega^\delta = \delta$. We prove

Theorem 3 **(Tree Conjecture).** — *Take any periodic trajectory δ of a triangle tiling billiard. Then the graph $G^\delta_\Delta := \Omega^\delta \cap \Lambda_\Delta$ (as a subgraph of Λ_Δ) is a* tree. *In other words, a trajectory δ passes by all the tiles that intersect its interior Ω^δ, see Figure 4.*

This proves a so-called Tree Conjecture that was first formulated in **[12]** and proven there for the case of tilings by *obtuse* triangles, a graph G^δ_Δ is in this case a chain. We also prove a generalization of this theorem for non-periodic trajectories, the so-called *Density property*. Although, the analogue of the Tree Conjecture for cyclic quadrilaterals is open.

Our interest in the Tree Conjecture comes from its relationship to the density properties of arithmetic and algebraic orbits of the Arnoux-Rauzy family, putting triangle tiling billiards in a larger perspective. These orbits are fractal curves related to the Peano curve studied in **[4]** by P. Arnoux, and another Peano curve studied in **[32]** by C. McMullen and in **[29]** by J. Lowenstein, G. Poggiaspalla and F. Vivaldi. We discuss more on these curves in paragraph **??**. It is possible that the trees we recover in this work are repelling real trees of the automorphisms of the corresponding free group , see **[15]**. Moreover, as a corollary of Theorem 3, with some additional work, we obtain that non-singular exceptional trajectories pass by all tiles in the triangle tiling.

1.3. Classification of billiard trajectories. — Take a triple of renormalized angles of a tile

$$(l_1, l_2, l_3) := \left(\frac{\alpha}{\pi}, \frac{\beta}{\pi}, \frac{\gamma}{\pi}\right) \in \Delta_2. \tag{2}$$

We now define a map on the set Δ_2 that can be seen as a map on triangle tilings. Let $l_j = \min\{l_k\}_{k=1}^3, j \in \mathcal{N}_\Delta := \{1, 2, 3\}$. Then one defines $(l'_1, l'_2, l'_3) \in \Delta_2$ via $l'_k := l_k - l_j$ for $k \neq j$ and $l'_j = l_j$, and subsequent rescaling. This algorithm is a **fully subtractive algoritm** and was studied in **[7]**. The fully subtractive algorithm is not well defined when $l_j = l_i$ for $i \neq j$. Let $\mathcal{E} \subset \Delta_2$ be the set of points ρ_Δ such that a corresponding (via (1) and (2)) triple of lengths (l_1, l_2, l_3) is a pre-image of a point $(1/3, 1/3, 1/3)$ under some iteration of the fully subtractive algorithm. We prove the following

Theorem 4 **(Classification of triangle tiling billiard trajectories.)** — *For any triangle tiling billiard, the following holds:*

1. *if $\rho_\Delta \notin \mathcal{R} \cup \mathcal{E}$ then any trajectory is either linearly escaping or periodic, and both behaviors are realized. Moreover, the set of symbolic codes realized by periodic trajectories is finite; there exist two functions $\omega_1, \omega_2 : \Delta_2 \setminus \mathcal{R} \cup \mathcal{E} \to \mathcal{A}_\Delta^{\mathbf{N}}$ such that the symbolic behaviour of any linearly escaping trajectory is an infinite word in the alphabet $\{\omega_1(\rho_\Delta), \omega_2(\rho_\Delta)\}$;*
2. *if $\rho \in \mathcal{R}$ then a trajectory escapes to infinity (is periodic) if and only if it passes (doesn't pass) through a circumcenter of a tile. Moreover, a list of symbolic codes of periodic trajectories is countable;*
3. *$\rho \in \mathcal{E}$ if and only if all the trajectories are periodic;*
4. *$\rho \in \mathbf{Q}^3 \setminus \mathcal{E}$ if and only if there exists a drift-periodic trajectory.*

The proof of this result is based on the connection of triangle tiling billiards with the set CET_τ^3 of fully flipped 3-interval exchange transformations defined in [**12**]. The set of squares of the maps in the family CET_τ^3 coincides with the set of real-rel deformations of the Arnoux-Rauzy maps. This helps us prove the following conjecture of P. Hooper and B. Weiss, from [**24**]: the arithmetic orbits of the Arnoux-Yoccoz map converge, up to rescaling, to the Rauzy fractal. The proof of this result, as well as that of Theorem 4, are based on two of our main tools - *tiling billiard foliations* and *renormalization in the family* CET_τ^3 that we describe in detail in the body of this work.

2. Plan of the article

This work is split into three parts. The first two parts cover on the dynamics of triangle tiling billiards. In the Part I, we study this dynamics from the geometric point of view. In Section 3 we remind the folding argument, in order to subsequently define tiling billiard foliations in Section 4. In Section 5 we prove the Tree Conjecture.

In the Part II, we study the dynamics of the family CET_τ^3 of fully flipped IETs. In Section 6, we remind the connection of their dynamics to that of the triangle tiling billiards as well as to real-rel leaves of the Arnoux-Rauzy surfaces and their arithmetic orbits. In Section 7 we introduce the renormalization process on CET_τ^3 and use it in order to characterize the symbolic dynamics. In Section 8 we give a complete classification of the billiard trajectories. In Section 9 we study the exceptional trajectories and show the convergence of arithmetic orbits of the Arnoux-Yoccoz map to the Rauzy fractal.

The Part III focuses on cyclic quadrilateral tiling billiards and open questions related to them, see Section 10. In the Appendix, we comment on our previous work [**25**] with P. Hubert.

PART I. ON A PROOF OF THE TREE CONJECTURE FOR TRIANGLE TILING BILLIARDS

A strategy of the proof of the Tree Conjecture is the following: the symbolic dynamics of any periodic trajectory is defined by a sequence of *flowers* (unions of singular leaves) in a periodic tiling billiard foliation.

3. Tiling billiards in locally foldable tilings

We present the folding construction proposed in [**12**] for triangle tiling billiards, in a slightly more general context. The **locally foldable tiling** is a two-colorable polygonal tiling of the plane such that the sum of the angles of tiles of one color around any vertex is equal to π. Obviously, both triangle and cyclic quadrilateral tilings are locally foldable.

Lemma 1. — *Consider any locally foldable tiling and some tile θ_0 in it. Let $\Lambda = (V, E)$ be a graph with V (E) being the set of vertices (edges) of tiles. Then there exists a unique map $\mathcal{F} = \mathcal{F}(\theta_0) : \mathbf{R}^2 \to \mathcal{F}(\mathbf{R}^2) \subset \mathbf{R}^2$ such that*

1. *for any tile θ the restriction $\mathcal{F}|_\theta$ is an isometry and $\mathcal{F}|_{\theta_0} = \mathrm{id}$;*
2. *for any two tiles θ and θ^e sharing an edge $e \in E$ their images $\mathcal{F}(\theta)$ and $\mathcal{F}(\theta^e)$ are symmetric one to each other with respect to a line bisector of $\mathcal{F}(e)$,*
3. *two different folding maps (with different θ_0) differ by a global isometry.*

Moreover, if the initial tiling is a triangle or cyclic quadrilateral tiling, then $\mathcal{F}(V) \subset \mathcal{C}$, where $\mathcal{C}$ is a circumcircle of the tile θ_0.

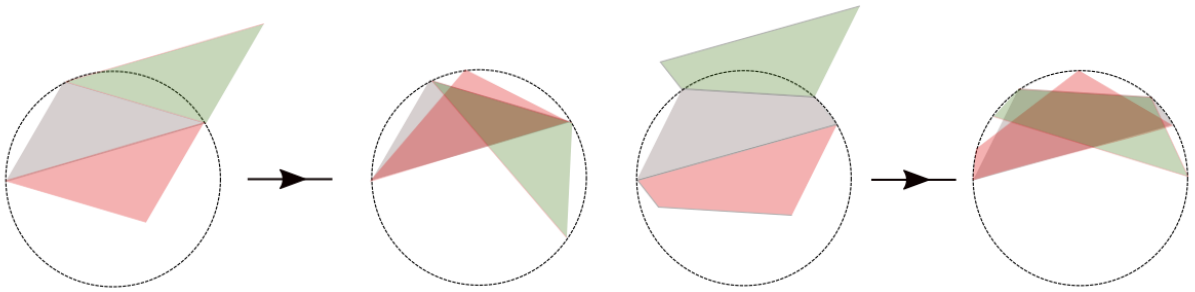

FIGURE 5. Folding on a circle for a patch of a triangle (and cyclic quadrilateral) tiling. A tile θ_0 maps to itself, and the other tiles map inside its circumcircle $\mathcal{C}$ under the folding map $\mathcal{F}(\theta_0)$.

Proof. — For any tile θ, we construct its image $\mathcal{F}(\theta)$ as follows. Take a **sequence** of tiles $\theta_0, \theta_1, \dots, \theta_n = \theta$ **connecting** θ_0 to θ: the tiles θ_k and θ_{k+1} share an edge. Then, fold the union $\theta_1 \cup \dots \cup \theta_n$ by a global isometry on θ_0. This defines $\mathcal{F}(\theta_1)$. Then, we fold $\theta_k \cup \dots \cup \theta_n$ on θ_{k-1} for $k = 2, \dots, n$. At the end of the process, one defines $\mathcal{F}(\theta)$ with $\mathcal{F}|_\theta$ an isometry.

It is left to prove that $\mathcal{F}(\theta)$ doesn't depend on the connecting sequence $\{\theta_k\}$, or equivalently, $\mathcal{F}(\theta_0) = \theta_0$ for any connecting **loop** ($\theta_0 = \theta_N$). First, when one folds one polygon on another in a tour around a vertex, the difference between the angles of positively and negatively oriented tiles in the vertex defines the displacement of the initial tile θ_0 with respect to its initial position. Since this difference is zero by definition, $\mathcal{F}\,|_{\theta_0} = \mathrm{id}$. By breaking any loop into a sum of loops around vertices, one finishes the proof. Clearly, two folding maps differ by an isometry.

Let us now prove that $\mathcal{F}(V) \subset \mathcal{C}$ for triangle and cyclic quadrilateral tilings. Indeed, $\mathcal{F}(v) \in \mathcal{C}$ obviously for the vertices of θ_0, and by folding for all the vertices of the tiles sharing an edge with θ_0. see Figure 5. Hence, $\mathcal{F}(v) \in \mathcal{C}$ for any $v \in V$ by recurrence. □

We call the map $\mathcal{F}$ a **folding map**, or simply, a **folding**. We call the image of the plane by a folding map a **bellow**, $\mathcal{B} := \mathcal{F}(R^2)$. A name *bellow* comes from accordeon bellows.

Remark 1. — The arguments of the above lemma are not new since the class of locally foldable tilings has been known for centuries in the origami community, see **[26]**, and also appeared recently in the discrete complex analysis for the dimer model **[2, 28, 14]**. In this paper we concentrate ourselves on triangle and cyclic quadrilateral tilings. We hope to develop the general theory of tiling billiards in locally foldable tilings in the future.

3.1. Basic orbit properties. — We generalize the proof from **[12]** given for triangle tiling billiards to any locally foldable tiling.

Theorem 5. — *The points 1.-3. of Theorem 1 hold for any locally foldable tiling.*

Proof. — Consider a trajectory δ of a tiling billiard starting in some tile θ_0, and a folding map $\mathcal{F} = \mathcal{F}(\theta_0)$. Then $\mathcal{F}(\delta)$ is a subset of a segment in the bellow $\mathcal{B}$ given by the intersection of $\mathcal{B}$ with some line l. Hence for any tile θ the intersection $l \cap \mathcal{F}(\theta)$ is equal to at most one segment. If δ is bounded then at some moment δ comes back to the same tile, and hence δ is periodic. Then, a periodic trajectory δ can't intersect itself in a transverse way inside a tile θ, since it intersects this tile in a *segment* equal to $\mathcal{F}^{-1}(\mathcal{F}(\theta) \cap l)$. Finally, a periodic trajectory is stable under a small enough perturbation since a sequence of tiles crossed by its perturbation δ' is the same as that for δ. Hence this sequence is a loop, and δ' is periodic with the symbolic dynamics of δ. □

Note. — In Hamiltonian dynamics, Arnold-Lioville integrability implies the existence of additional integrals of motion. For tiling billiards, the direction of a trajectory in folded coordinates is a first integral. The folding map reduces the dimension of the phase space.

4. Tiling billiard foliations

Take any locally foldable tiling, fix a tile θ_0 in it and a folding $\mathcal{F}$. Slice up the bellow $\mathcal{B}$ by either a family of *parallel* chords, or a family of chords *emanating from one point* and pull this slicing back to the tiled plane by $\mathcal{F}^{-1}$. This defines two families of *foliations* on the tiled plane, and any trajectory can be included as a leaf of these foliations.

4.1. When hitting a corner. — In a classic setting of billiards in bounded domains with piecewise smooth boundary, a billiard trajectory that arrives to a non-regular point on the boundary is not well-defined. In the context of tiling billiards in locally foldable tilings, one can correctly define, although possibly branching, singular trajectories as boundaries of cylinders of parallel trajectories.

A piece-wise linear simple curve γ on the tiled plane that passes through at least one vertex of a tiling is called a **singular trajectory (a separatrix)**, if the Snell's refraction law with coefficient $k = -1$ holds in all non-regular points of such a trajectory. We call the segment $\theta \cap \gamma$ of a singular trajectory γ in the tile θ a **separatrix segment** if $\gamma \cap \theta \cap V \neq \emptyset$, i. e. γ passes by a vertex of θ. If a singular trajectory is a closed curve, we call it a **separatrix loop**.

Consider a singular trajectory γ with a singular point $v \in V$. One associates to it a finite number of singular trajectories passing by v, via folding. Indeed, γ folds into some chord l in the bellow such that $l \cap \mathcal{F}(V) \neq \emptyset$. One considers all of the connected components of the set $\mathcal{F}^{-1}(l \cap \mathcal{B}) \setminus \{v\}$ such that their intersection with the set $\Theta_v := \cup_{\theta : \theta \ni v} \theta$ is non-empty. These connected components (eventually united with a point $\{v\}$) are exactly the separatrix curves passing by v that fold into the same chord as γ. We call the union of *all* separatrices passing by a fixed vertex $v \in V$ and mapping to the same chord under folding, a **flower** in v. We call each of the separatrix loops in one flower a **petal** of this flower. We call $v \in V$ a **pistil**. A flower is **bounded** if all of its separatrices are petals. To any line l such that $\mathcal{F}(V) \cap l \neq \emptyset$, one may associate a flower.

4.2. Parallel and ray foliations. — From now on, we restrict ourselves to the case of triangle or cyclic quadrilateral tilings. Fix some base tile θ_0 and a corresponding folding map $\mathcal{F}$. Then the bellow $\mathcal{B}$ is a subset of the disk $\mathcal{D}$, $\partial\mathcal{D} = \mathcal{C}$.

Take $\tau \in \mathbb{S}^1$ and consider a foliation of the plane by parallel lines with a common direction $\exp(i\tau)$. One considers the intersections of the leaves of this foliation with the bellow $\mathcal{B}$. Then, by applying $\mathcal{F}^{-1}$ to these intersections, one obtains a **parallel foliation** $\mathcal{P}_\tau$ (or simply, $\mathcal{P}$) of the plane with a tiling. Now take a point $p \in \mathcal{C}$. Consider all the chords in $\mathcal{D}$ passing by p, slicing up the bellow $\mathcal{B}$. By unfolding these slices back to the plane with a tiling one obtains the **ray foliation** $\mathcal{R}_p$ (or simply, $\mathcal{R}$). The set $\mathcal{F}^{-1}(p)$ is non-empty if and only if $p = \mathcal{F}(v)$ for some $v \in V$. Moreover, if the angles of tiles are ratinonally independent, in this case $\mathcal{F}^{-1}(p) = \{v\}$. It will be sufficient for us to study the ray foliations with $p \in \mathcal{F}(V) \subset \mathbb{S}^1$.

Lemma 2. — *Fix a tile θ_0 in a triangle (cyclic quadrilateral) tiling. Fix $\tau \in \mathbb{S}^1$ and $p \in \mathcal{C} \simeq \mathbb{S}^1$ such that $p = \mathcal{F}(v)$ for some $v \in V$. Then, the following holds for the foliations $\mathcal{P}_\tau$ and $\mathcal{R}_p$:*

1. *the foliations $\mathcal{P}_\tau$ and $\mathcal{R}_p$ are well defined and orientable. Moreover, their oriented connected leaves define tiling billiard trajectories;*
2. *the set of singularities for both foliations coincides with the set V;*
3. *for any $v \in \mathcal{F}^{-1}(p)$, there exist finitely many separatrices in $\mathcal{P}_\tau$ passing by v, at most one by each tile $\theta \subset \Theta_v$. Two separatrices through v in $\mathcal{P}_\tau$ belong to the same flower;*
4. *take any (possibly singular) trajectory δ. Then there exists a unique τ such that δ is a leaf of $\mathcal{P}_\tau =: \mathcal{P}^\delta$. If δ folds into a chord l such that intersects $l \cap \mathcal{F}(V) \neq \emptyset$, then δ can be also included in a radial foliation $\mathcal{R}_p =: \mathcal{R}^\delta$ for each (of at most two) $p \in \mathcal{F}(V) \cap l$;*
5. *for any periodic trajectory δ its interior Ω^δ is foliated by the leaves of $\mathcal{P}^\delta$ (and of $\mathcal{R}^\delta$).*

Proof. — This is a simple corollary of Lemma 1 and Theorem 5. If a tile θ_0 is positively oriented, then the orientation of $\mathcal{R}_p$ and $\mathcal{P}_\tau$ coincides with (is opposite to) the orientation of sheaves of lines on the bellow on positively (negatively) oriented triangles. □

4.3. Local behavior of flowers. — The following proposition describes the local combinatorics of flowers on periodic triangle tilings.

Proposition 1. — *Fix $v \in V$, a tile $\theta_0 \ni v$ and $\tau \in \mathbb{S}^1$. This defines a flower γ in $\mathcal{P}_\tau$ with a pistil in $v \in V$. Denote by $s \in \mathbf{N}$ the number of its separatrix segments containing v. Then $s \in \{0, 2, 4, 6\}$ and each tile $\theta \subset \Theta_v = \cup_{\theta \ni v} \theta$ contains at most one separatrix segment of γ. Moreover, up to a possible change of orientation $\tau \mapsto -\tau$, the set $\gamma \cap \Theta_v$ has one of the combinatorial behaviors represented on Figure 6.*

Proof. — Finiteness of s follows from the point 3. in Lemma 2, and s is even since the foliation $\mathcal{P}_\tau$ is oriented. The separatrices passing by v are leaves of both $\mathcal{P}_\tau$ and $\mathcal{R}_p$ with $p = \mathcal{F}(v)$. Moreover, the ray foliation $\mathcal{R}_p$ has a very simple form in restriction to the union Θ_v: all of its leaves pass by v and their directions alternate from one tile to its neighbor. This finishes the proof. □

The list given in Proposition 1 is realizable although not necessarily by bounded flowers. Moreover, the analogous statement can also be proven for quadrilateral tilings.

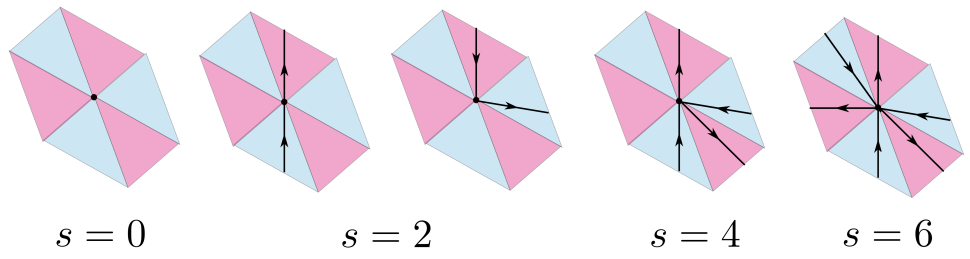

FIGURE 6. *All possible behaviors of restrictions of a flower γ on the set Θ_v.* This Figure contains the information on the number of separatrix segments and their relative positions.

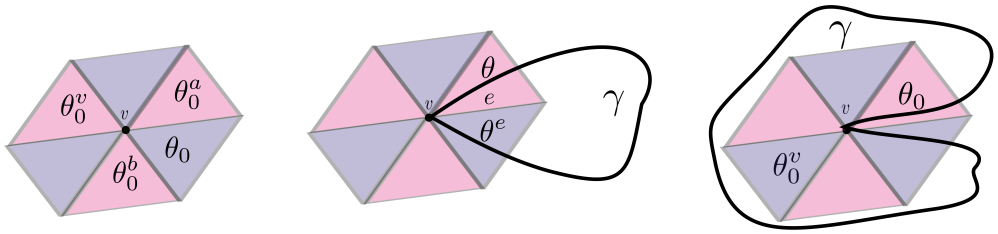

FIGURE 7. *Different notations relative to flowers in triangle tilings.* First, the neighbouring tiles θ_0^a (sharing an edge a) and θ_0^b (sharing an edge b) as well as the opposite tile θ_0^v to the tile θ_0; second, a loop γ satisfying the Flower Conjecture passes by θ and θ^e and the set Ω^γ contains the edge e; third, a petal of a hungry flower γ passes by a tile θ_0 and the opposite tile θ_0^v is contained inside Ω^γ.

5. Proof of the Tree Conjecture

We give a proof of the Tree Conjecture by first reducing it to the Bounded Flower Conjecture.

5.1. Flower Conjecture. — Let us introduce some notations. Two tiles are **neighbouring in** e if they share an edge e and **opposite in a vertex** v if they both pass by v and are centrally symmetric to each other with respect to v. For any tile θ_0, $e \in E, v \in V$ such that $e \subset \theta_0, v \in \theta_0$ we denote by θ_0^e its neightbouring tile in e, and by θ_0^v its opposite tile in v, see Figure 7.

The **Flower Conjecture holds for a petal** γ if for any $v \in \gamma \cap V$, there exists $e \in E$ such that $v \in e \subset \Omega^\gamma$, and γ passes by the tiles θ and θ^e, see Figure 7. The **Flower conjecture holds for a tiling** if it holds for all the possible petals. The **Bounded Flower Conjecture holds for a tiling** if the Flower Conjecture holds for all possible petals of bounded flowers.

Obviously, the Flower Conjecture implies the Bounded Flower Conjecture. The Flower Conjecture also implies that two petals γ_1 and γ_2 of the same flower have the same index and the domains $\mathring{\Omega}^{\gamma_1}$ and $\mathring{\Omega}^{\gamma_2}$ are disjoint. Theorem 7 excludes petals passing by two opposite triangles, as well as petals passing by neighbouring triangles but not contouring an edge between them, see Figure 10.

Theorem 6. — *The Bounded Flower Conjecture holds for all periodic triangle tilings.*

Theorem 7. — *The Flower Conjecture holds for all periodic triangle tilings.*

Of course, the second theorem is a stronger version of the first. We reduce the Tree Conjecture to Theorem 6 and postpone the proof of Theorem 7 to Section 10. The Tree Conjecture can be formulated for any locally foldable tiling (and we denote by G^δ a subgraph of the tiling graph bounded by a trajectory δ) even though it doesn't always hold, e.g. it breaks for a triangle tiling with six additional tiles cut out by a triangle tiling billiard trajectory.

Proposition 2. — *For any locally foldable tiling, the Bounded Flower Conjecture is equivalent to the Tree Conjecture.*

Proof. — Suppose that the Bounded Flower Conjecture fails for the petals $\gamma_j, j \in J$ of some flower γ with a pistil $v \in V$. Take all of the petals γ_i that are not contained in Ω^{γ_j} for some $j \in J, j \neq i$, with indices in a subset $J_0 \subset J$. Then there exists a periodic trajectory δ passing by the same tiles as $\cup_{j \in J_0} \gamma_j$, with $\cup_{j \in J_0} \Omega^{\gamma_j} \subset \Omega^\delta$, that contours a tile.

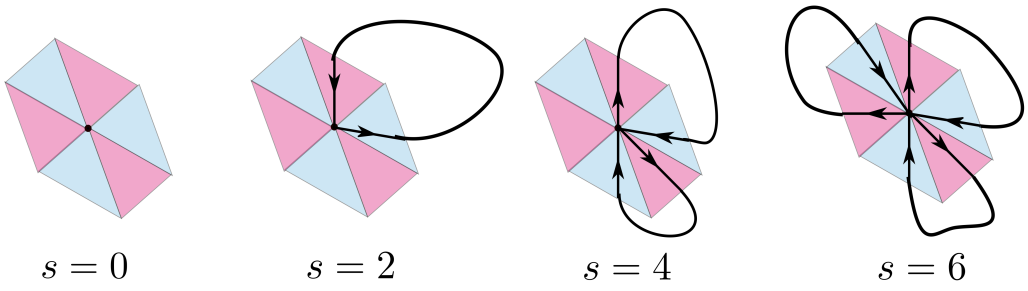

FIGURE 8. *Possible behaviors of bounded flowers on periodic triangle tilings.*

Suppose now that the Bounded Flower Conjecture holds. Take a periodic trajectory δ. Then the domain Ω^δ is foliated by the leaves of $\mathcal{P}^\delta$, among which only a finite number of singular ones. We contract δ in $\mathcal{P}^\delta$ in a direction of the inner normal to $\partial\Omega^\delta$, in order to obtain a flower γ with a singularity in some vertex $v \in \Omega^\delta \cap V$. If $\gamma = \{v\}$, then $G^\delta = \gamma$ and Tree Conjecture obviously holds.

Suppose now that δ contracts to a non-trivial flower γ. We can assume that such flower has its only singularity in $v \in V$. If not, under folding γ maps into a chord l between $\mathcal{F}(v)$ and $\mathcal{F}(v'), v, v' \in V, v \neq v'$. But then we perturb the initial direction of δ to obtain a trajectory δ' with the same symbolic dynamics, in such a way that a perturbed chord l' such that $\mathcal{F}(\delta') \subset l'$, passes by v but doesn't pass by v'. This can be done since the set $\mathcal{F}(V)$ is countable.

Thus we obtain a flower γ with a pistil in $v \in V$ with $m \in \mathbf{N}$ petals (m is bounded by the half of the valency). Now we approach each of the petals γ_j by periodic leaves $\delta_j \subset \Omega^{\gamma_j}$ in $\mathcal{P}^\gamma$. Then$G^\delta_\Delta = \cup_j G^{\delta_j}_\Delta \cup e_j$, where e_j are the edges passing through v inside each of the petals γ_j. Such a recurrence process eventually stops since the period of δ_j diminishes. □

Example. — The proof of Proposition 2 is constructive. The graph G^δ is built as a growing union of finite graphs, $G^\delta = \cup_{k=1}^K G_k$. On the step k one adds to the graph G_k the pistils of new flowers with the edges inside the petals of these new flowers connected to these pistils. Any vertex $v \in \Omega^\delta \cap V$ is a pistil of a flower on some step, by Lemma 2.

5.2. Obstructions to the Bounded Flower Conjecture for triangle tilings. — Till the end of this Section, we only study the periodic triangle tiling and only bounded flowers in it. We denote flowers by γ, and their petals by the same letter with indices.

The only cases of global behavior of flowers contradicting the Bounded Flower Conjecture while respecting Proposition 1 are enumerated on Figure 9 and in the following list in which we stress the set $\mathcal{O}$ of petals for which the Bounded Flower Conjecture fails.

Flower obstructions to the Bounded Flower Conjecture for triangle tilings.

- **2.1.** A flower has one petal γ_1 that passes by a pair of opposite tiles, $\mathcal{O} = \{\gamma_1\}$.
- **2.2.** The only petal γ_1 passes by a pair of neighbouring tiles in e but $e \notin \Omega^{\gamma_1}$, $\mathcal{O} = \{\gamma_1\}$.
- **4.1.** A flower has two petals of different indices as curves. For **4.1a** and **4.1b**, a petal γ_1 passes by opposite tiles and a petal γ_2 passes by two neighbouring tiles: **4.1a.** $\Omega^{\gamma_2} \subset \Omega^{\gamma_1}$ and $\mathcal{O} = \{\gamma_1\}$, **4.1b.** $\Omega^{\gamma_1} \subset \Omega^{\gamma_2}$ and $\mathcal{O} = \{\gamma_2\}$). **4.1c.** Both petals γ_1 and γ_2 pass by neighbouring tiles, $\Omega^{\gamma_1} \subset \Omega^{\gamma_2}$ and $\mathcal{O} = \{\gamma_2\}$.
- **4.2.** The petals γ_1 and γ_2 have the same index, γ_1 passes by opposite triangles, $\mathcal{O} = \{\gamma_1\}$.
- **6.1.** A flower has three petals, the petal γ_3 passes by opposite triangles,$\Omega^{\gamma_2} \subset \Omega^{\gamma_3}$, $\mathcal{O} = \{\gamma_3\}$.
- **6.2.** The three petals γ_1, γ_2 and γ_3 are such that $\Omega^{\gamma_3} \subset \Omega^{\gamma_2} \subset \Omega^{\gamma_1}$, and $\mathcal{O} = \{\gamma_1, \gamma_2\}$.
- **6.3.** All three petals γ_1, γ_2 and γ_3 pass by neighbouring tiles, $\Omega^{\gamma_1} \cup \Omega^{\gamma_2} \subset \Omega^{\gamma_3}, \mathcal{O} = \{\gamma_3\}$.

The first number in the name of the obstruction is the number of separatrix segments. This list is given modulo a possible change of orientations of all the petals. Without loss of generality, we fix the orientations as shown on Figure 9. We now prove that these obstructions are never realized by triangle tiling billiard trajectories. We first present our main tools.

In order to prove Theorem 6, we use two properties specific to a periodic triangle tiling. First, we use the *square property* from point 5. in Theorem 1 which is a corollary of the renormalization process we introduce in the second part. We postpone the proof of this property to the paragraph 8.1. Second, we use the *symmetry* of the ray foliation $\mathcal{R}_p$ for $p = \mathcal{F}(v), v \in V$. Neither of these properties holds for cyclic quadrilateral tilings.

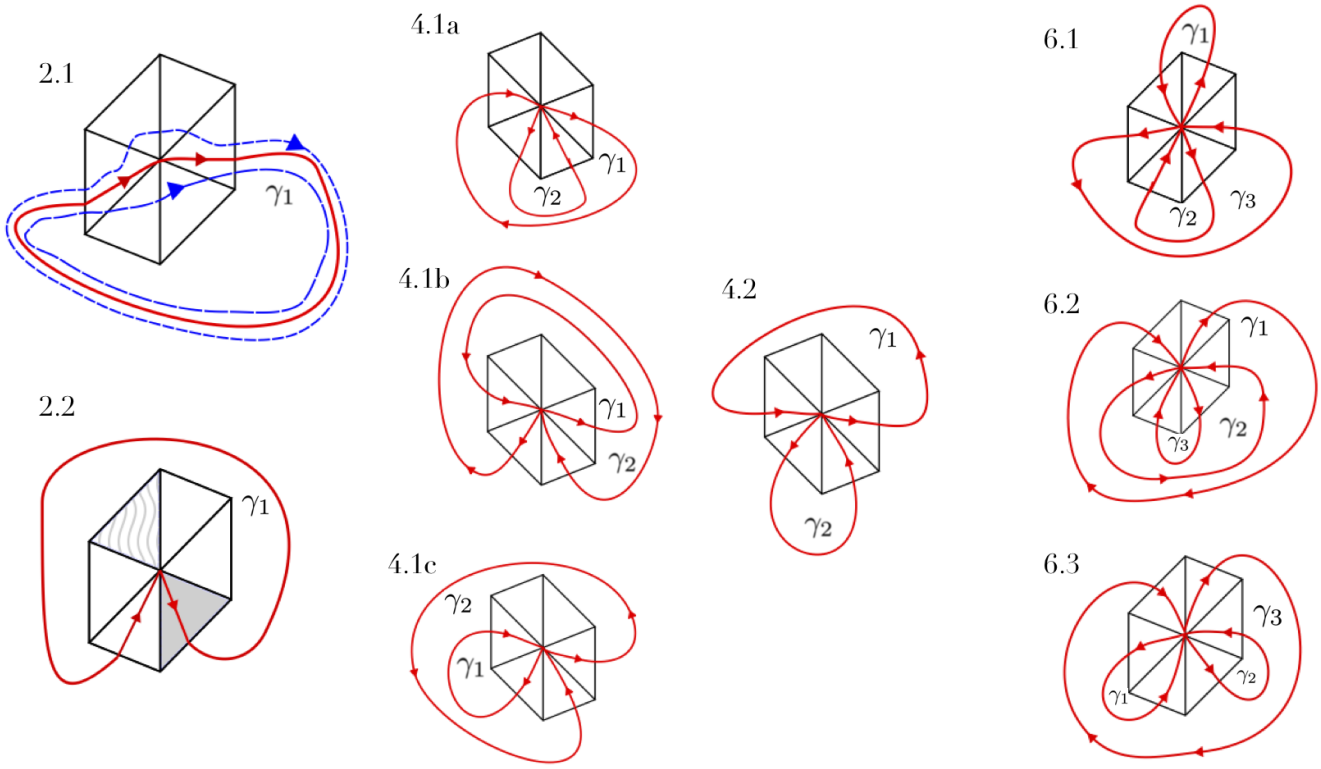

FIGURE 9. *A list of topological obstructions for the Bounded Flower Conjecture.* This Figure carries the combinatorial information on the intersection $\gamma \cap \Theta_v$ and the topological information on global behavior.

5.3. Exclusion of obstructions for one petal flowers. — We now show in detail how to exclude the cases **2.1** (via the square property) and **2.2** (via the symmetry of the ray foliation), and treat all the other cases in the next paragraph.

Define a sign alphabet $\mathcal{S} := \{+, -\}$ and a sign map $\sigma : \mathcal{A}^2_\Delta \to \mathcal{S}$ explicitely by $\sigma(ab) = \sigma(bc) = \sigma(ca) = +$ and $\sigma(ba) = \sigma(cb) = \sigma(ac) = -$. This sign map extends to the map $\sigma : \left(\mathcal{A}^2_\Delta\right)^{\mathbf{N}} \to \mathcal{S}^{\mathbf{N}}$ that we denote by the same letter. This map simplifies an accelerated symbolic code into a **sign code**.

We consider the (accelerated) symbolic codes of periodic trajectories as *cyclic words*, i.e. for us the two periodic words $w_0 \dots w_n$ and $w_k w_{k+1} \dots w_n w_0 \dots w_{k-1}$ are equal for any $j, k \in \{0, 1, \dots, n\}, k \neq 0$ and any $w_j \in \mathcal{A}^2_\Delta$.

Example. — The accelerated (cyclic) symbolic code of a 6-periodic orbit is $(ab\ bc\ ca)^2 = (bc\ ca\ ab\ )^2$. Its corresponding sign code in both cases is $(+\,+\,+)^2$.

In the following, we denote by γ_j the petals and by δ_j the periodic trajectories approaching these petals or their unions. We identify the trajectories with their symbolic orbits, i.e. we denote by the same letter a closed curve on the plane as well as a corresponding cyclic periodic word in the alphabets $\mathcal{A}^2_\Delta$ or $\mathcal{S}$.

Proposition 3. — *A configuration **2.1** is never realized by a bounded flower.*

Proof. — Suppose that a configuration **2.1** is realized by a one-petal flower γ_1 in the vertex v. We now perturb γ_1 in the foliation $\mathcal{P}^{\gamma_1}$ in order to obtain two periodic trajectories δ_{in} and δ_{out} in a small neighbourhood of γ_1 with $\delta_{\text{in}} \subset \Omega^{\gamma_1}$ and $\delta_{\text{out}} \nsubseteq \Omega^{\gamma_1}$, see Figure 10.

Suppose that outside the set Θ_v the trajectories $\delta_{\text{in}}, \delta_{\text{out}}$ and γ_1 pass by the same tiles. Then there exists a word $S \in \mathcal{S}^{\mathbf{N}}$ of even length such that the sign codes of δ_{in} and δ_{out} are: $\delta_{\text{in}} = +--+S$ and $\delta_{\text{out}} = -++-S$. We split $S = s\bar{s}$ into a concatenation of two words of equal length, $s, \bar{s} \neq \emptyset$. Then $\delta_{\text{in}} = -+s\bar{s}+-$ and $\delta_{\text{out}} = +-s\bar{s}-+$.

But since the words δ_{in} and δ_{out} are squares of some words in the alphabet $\mathcal{S}$, length considerations give that simultaneously $-+s = \bar{s}+-$ and $+-s = \bar{s}-+$. These two equations imply that the word s finishes by $+$ and $-$ at the same time, which is a contradiction. □

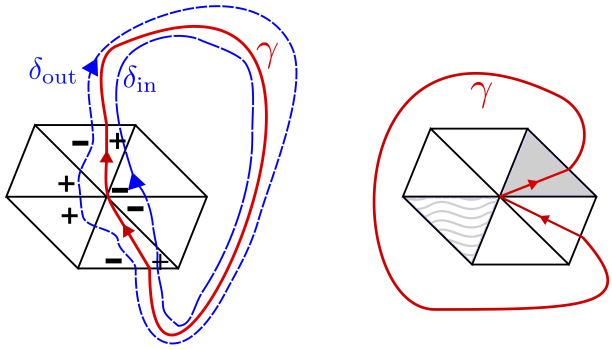

FIGURE 10. *Obstructions to the Flower Conjecture and illustrations for the proofs.* First, for a petal γ, two possible obstructions for the Flower Conjecture; second, if γ is an only petal in its bounded flower, then these are the obstructions **2.1** and **2.2**; third, illustration for the proofs of Propositions 3 and 4.

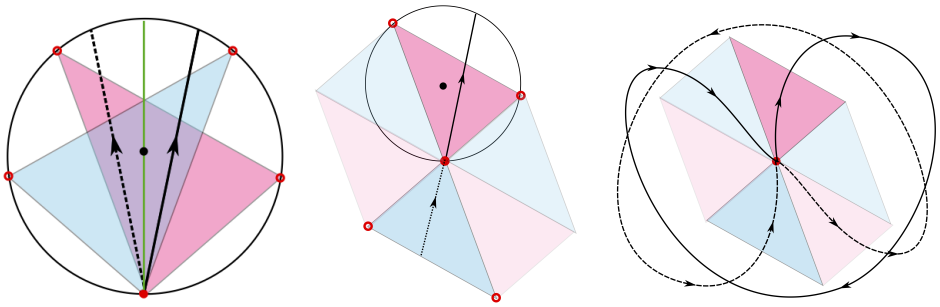

FIGURE 11. *Symmetry of the ray foliation $\mathcal{R}_p$ with $p = \mathcal{F}(v), v \in V$.* First, folded triangles $\mathcal{F}(\theta_0)$ and $\mathcal{F}(\theta_0^v)$ symmetric to each other with respect to the diameter $d \ni p$; then, associated unfolded segments and third, a hungry flower γ and its opposite γ^v.

Now we observe that for the case **2.2** a following property holds. There exists a petal γ_1 and a tile $\theta_0 \ni v$ such that $\gamma_1 \cap \theta_0 \neq \emptyset$ and $\theta_0^v \subset \Omega^{\gamma_1}$. In this case, we say that the tile θ_0 is a **hungry tile** and that it eats up θ_0^v. We call a flower γ (not necessarily bounded) a **hungry flower** if there exists a petal in this flower passing by a hungry triangle, see Figure 7.

Proposition 4. — *1. The ray foliation $\mathcal{R}_p$ with $p = \mathcal{F}(v), v \in V$ is centrally symmetric with respect to v, modulo a change of orientation of leaves in opposite tiles. 2. A configuration of separatices forming a hungry flower is never realized by triangle tiling billiard foliations.*

Proof. — For any separatrix segment of the trajectory γ_0 starting in a vertex v and in the tile $\theta_0 \ni v$, consider a separatrix segment starting in v and crossing the tile θ_0^v such that it belongs to the same line as the initial segment. By symmetry, the corresponding trajectory γ_0^v is centrally symmetric to γ_0 with respect to v, and has different orientation. This proves 1.

Consider now a hungry flower γ in the vertex v and include it in its ray foliation $\mathcal{R}^\gamma$. This foliation contains a symmetric flower γ^v defined as in the proof of point 1 by symmetry. The hungry flower configuration implies that these two flowers γ and γ^v intersect outside v. This is not possible since γ and γ^v are leaves of the same foliation, see Figure 11. □

Note. — The two tiles θ_0 and θ_0^v fold into two triangles in the bellow, symmetric with respect to the diameter d of the circle $\mathcal{C}$ such that $d \ni \mathcal{F}(p)$. The corresponding symmetric trajectories γ_0 and γ_0^v constructed in the proof of the above Proposition 4 fold into the chords symmetric with respect to the same diameter d, see Figure 11. In the ray foliation $\mathcal{R}_p$ the trajectories crossing θ_0 (θ_0^v) go out of (into) v.

Corollary 1. — *Configurations **2.2, 4.1c, 6.2** and **6.3** are never realized by bounded flowers.*

Proof. — All these configurations form hungry flowers and by Proposition 4, are never realized. □

5.4. Exclusion of remaining cases and finalisation of the proof. — All of the remaining cases are excluded with the use of the square property.

Proposition 5. — *Configurations **4.1a** and **4.1b** are never realized by bounded flowers.*

Proof. — Consider the case **4.1a**. We denote $\gamma_{\text{in}} := \gamma_2$ and $\gamma_{\text{out}} := \gamma_1$. We approach γ_{in} by a trajectory $\delta_1, \delta_1 \subset \Omega^{\gamma_{\text{in}}})$, and γ_{out} by a trajectory $\delta_2, \delta_2 \subset \mathbf{R}^2 \setminus \Omega^{\gamma_{\text{out}}}$. One can choose a trajectory $\delta, \delta \subset \Omega^{\gamma_{\text{out}}} \setminus \Omega^{\gamma_{\text{in}}}$ close enough to the boundary, in such a way that it passes by the same tiles as $\gamma_{\text{in}} \cup \gamma_{\text{out}}$. All of the trajectories $\delta_1, \delta_2, \delta$ are chosen to be periodic, non-singular and belong to the same foliation $\mathcal{P}^\gamma$. Then there exist the words $w, u \in \mathcal{S}^{\mathbf{N}}$ such that

$$\begin{aligned} \delta_1 &= (w--)^2, \\ \delta_2 &= (u-++-)^2, \\ \delta &= ++w--w++u-++-u. \end{aligned}$$

Since δ is a symbolic square, and from length considerations, we obtain the word equality $-w++u-+= +-u++w-$ which is impossible since $- \neq +$. The argument for the case **4.1b** is the same, with $\gamma_{\text{in}} := \gamma_1$ and $\gamma_{\text{out}} := \gamma_2$. □

Proposition 6. — *Configuration **4.2** is never realized by a bounded flower.*

Proof. — Define three non-singular periodic trajectories δ_1, δ_2 and δ in the parallel foliation $\mathcal{P}^\gamma$. First, $\delta_j \in \Omega^{\gamma_j}$ and δ_j passes by the same tiles as γ_j for $j = 1, 2$. Then, we take a trajectory δ that passes by the same tiles as the flower γ and such that $\gamma \subset \Omega^\delta$. Then, there exist the words $s, \bar{s}, w \in \mathcal{S}^{\mathbf{N}}$ such that the words s and $\bar{s}$ have equal length and

$$\begin{aligned} \delta_1 &= -++-s\bar{s}, \\ \delta_2 &= (--w)^2, \\ \delta &= ++w--w++s\bar{s}. \end{aligned}$$

Length considerations imply the following two equations: $\bar{s}-+=+-s$ and $-w++s = \bar{s}++w-$. These two are incompatible, since the word s has to finish by $-$ and $+$ simultaneously. □

Proposition 7. — *Configuration **6.1** is never realized by a bounded flower.*

Proof. — We choose periodic non-singular trajectories $\delta_1, \delta_2, \delta_3$ and δ_4 as follows. First, the trajectories δ_j pass by the same tiles as γ_j and $\delta_j \subset \Omega^{\gamma_j}$ for $j = 1, 2$; second, a trajectory δ_3 is close to the boundary $\partial\left(\Omega^{\gamma_1} \cup \Omega^{\gamma_3}\right) \subset \Omega^{\delta_3}$; third, a trajectory $\delta_4 \subset \Omega^{\gamma_3} \setminus \Omega^{\gamma_2}$ and is close to its boundary. Then there exist the words $w, v, U \in \mathcal{S}^{\mathbf{N}}$ such that

$$\begin{aligned} \delta_1 &= (w--)^2, \\ \delta_2 &= (v++)^2, \\ \delta_3 &= ++w--w++U, \\ \delta_4 &= --v++v--U. \end{aligned}$$

Since both δ_3 and δ_4 are symbolic squares, one can split the word U in two words $u, \bar{u} \in \mathcal{S}^{\mathbf{N}}$ of equal length, $U = u\bar{u}$. The length considerations for δ_3 and δ_4 imply that $-w++u = \bar{u}++w-$ and $\bar{u}--v-=+v--u$. Since the word $\bar{u}$ can't start from $+$ and $-$ at the same time, we have a contradiction. □

Theorem 6 now follows. Indeed, for any bounded flower γ with a pistil in $v \in V$ one can suppose that v is the only singularity of γ, see the proof of Proposition 2. From all of the above follows that γ satisfies the Bounded Flower Conjecture. By Proposition 2, this finishes the proof of Theorem 3. Our strategy also gives a new proof of the following

***Proposition 8* ([12]).** — *A periodic trajectory on an obtuse triangle tiling encloses a* path.

Proof. — Any flower in some vertex $v \in V$ in an obtuse tiling has *at most two* petals (and this implies that contoured trees are paths). It follows from applying the folding map to Θ_v. One simply verifies that $\mathcal{F}\left(\theta_\alpha^v\right) \cap \mathcal{F}\left(\theta_\alpha\right) = \{p\}$ and $\mathcal{F}\left(\theta_\beta^v\right) \cap \mathcal{F}\left(\theta_\beta\right) = \{p\}$, see Figure 12. Here $\theta_\bullet, \bullet \in \{\alpha, \beta, \gamma\}$ is a tile in Θ_v with an angle $\bullet$ in v. Hence a flower in v can't simultaneously pass by the interior of the tiles θ_α and θ_α^v (the same for θ_β and θ_β^v). □

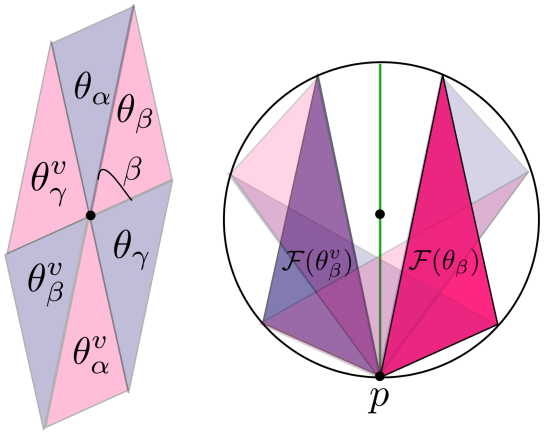

FIGURE 12. *Folding of Θ_v in the obtuse triangle tiling.* First, the notations for the tiles $\theta_\bullet$. Second, the images of opposite tiles with acute angle in v intersect only in $p = \mathcal{F}(v)$.

Triangle tiling billiards	CET^3_τ (*and translation*)
angles of a tile α, β, γ	parameters $(l_1, l_2, l_3) \in \Delta_2$ (*via rescaling* (2))
oriented distance d from a segment of a trajectory to the circumcenter of a tile	$\tau \in \mathbb{S}^1$ (*via* $d = \cos \pi\tau$, *see* [Proposition 1, **[25]**])
relative position of a tile with respect to the folded trajectory	$p \in \mathbb{S}^1$ (*via folding* $\mathcal{F}$)
starting tile θ_0 of fixed orientation	$p_0 \in \mathbb{S}^1$ (*via folding*, $p_0 \in \mathcal{F}(\theta_0) \cap \mathcal{C}$)
the set V of vertices and a corresponding set $\mathcal{F}(V)$	$\mathcal{C}(p_0) := \{n\alpha + m\beta + p_0, n, m \in \mathbb{Z}\}$ (*by identification* $\mathcal{C} \simeq \mathbb{S}^1$)
ray foliation $\mathcal{R}_{p_0}$ with $p_0 = \mathcal{F}(v_0)$	action of a subfamily with fixed $(l_1, l_2, l_3) \in \Delta_2$ and varying τ, on the subset $\mathcal{C}(p_0) \subset \mathbb{S}^1$
parallel foliation $\mathcal{R}_\tau, \tau \in \mathbb{S}^1$	action of a subfamily with fixed $(l_1, l_2, l_3) \in \Delta_2$ and varying $\tau(\varepsilon)$, on the set $\mathcal{C}(p(\varepsilon))$, here $\tau(\varepsilon) = \tau_0 + 2\varepsilon$ and $p(\varepsilon) = p_0 + \varepsilon$

TABLE 1. Vocabularly between the triangle tiling billiards dynamics and that of the maps in CET^3_τ.

PART II. RENORMALIZATION FOR FULLY FLIPPED 3-INTERVAL EXCHANGE TRANSFORMATIONS

6. Fully flipped interval exchange transformations and their squares

6.1. Definition of the family CET^n_τ. — Fix $(l_1, \dots, l_n) \in \Delta_n := \{(l_1, \dots, l_n) \in \mathbf{R}^n_+ \mid l_1 + \dots + l_n = 1\}$. Cut the circle $\mathbb{S}^1$ of length 1 into n disjoint intervals $I_j, |I_j| = l_j$. Define a map $F_0 : \mathbb{S}^1 \to \mathbb{S}^1$ as a composition of n (commuting) involutions on each one of these intervals. We say that a map F **belongs to the family** CET^n_τ if $F = R_\tau \circ F_0$, where R_τ is an angle $\tau \in \mathbb{S}^1$ rotation . In the following we often write $F = F^{l_1,\dots,l_n}_\tau$ in order to stress the corresponding parameters. Note that the map $F = R_{1/2} \circ F_0$ is a composition of two non-commuting involutions. The symbolic dynamics of the map $F \in \mathrm{CET}^n_\tau$ is defined in a standard way as a map from $\mathbb{S}^1$ to $\{1, \dots, n\}^{\mathbf{N}}$ associating to each point the labels of intervals visited by its orbit $\{F^{\circ k}(p)\}_{k \in \mathbf{N}}$.

The dynamics of a triangle (cyclic quadrilateral) tiling billiard trajectory can be reduced to the study of a map in CET^3_τ (or CET^4_τ). For triangle tilings, it has been proven in **[12]** by inducing the dynamics of the billiard to that on the circumcircle $\mathcal{C}$ via folding, see **[12, 25]** for more details. We summarize the connection between triangle tiling billiards and the family CET^3_τ in the vocabularly in the Table 1, for the most part established in **[12]**. We add to it the two last lines.

Analogously, to any cyclic quadrilateral, one associates a subfamily of maps in CET^4_τ is defined by the lengths

$$(l_1, l_2, l_3, l_4) = \left(\frac{\alpha_1}{\pi}, \frac{\gamma_2}{\pi}, \frac{\gamma_1}{\pi}, \frac{\alpha_2}{\pi}\right), \tag{3}$$

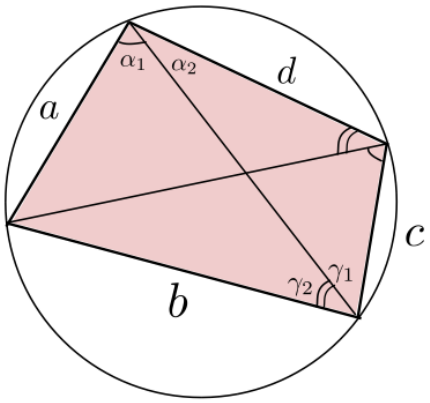

FIGURE 13. *Cyclic quadrilateral and the angles* $\alpha_1, \alpha_2, \gamma_1, \gamma_2$. These angles define the angles $\alpha, \beta, \gamma, \delta$ via the relations: $\alpha_1 + \alpha_2 = \alpha, \beta = \gamma_1 + \alpha_2, \gamma = \gamma_1 + \gamma_2, \delta = \alpha_1 + \gamma_2$.

where the angles on the right in (3) are those in which the diagonal of a tile splits the opposite angles of the quadrilateral, see Figure 13. Any cyclic quadrilateral is defined by such a quadruple of angles up to homothety, even though it is not uniquely defined by its angles $\alpha, \beta, \gamma, \delta$.

In the following, we study the dynamics (symbolic dynamics) of the family CET^3_τ which reunites the dynamics of the rel deformations of Arnoux-Rauzy surfaces and that of the triangle tiling billiards. The question of symbolic dynamics in the family CET^n_τ can be studied for *any* n. In this work, we concentrate on the case of the maps in CET^3_τ simply because it is the only case that we were able to treat. See Section 10 for the discussion of the case $n \geq 4$ and related open questions.

6.2. Square roots of the Arnoux-Rauzy maps. — By a classical Keane's Theorem proven in **[27]**, almost every n-interval exchange transformation (IET) with irreducible combinatorics is minimal. An interesting question and open question is to study the minimality in the *k-parametric families of n-IET* for $k < n$. Many recent works give partial answers, e.g. **[38, 11]**.

Let us remind the definition of the **Arnoux-Rauzy family** $\mathrm{AR}(\mathbb{S}^1)$ of 6-IETs on the circle of unit length, with parameters in the 2-simplex. Cut the circle $\mathbb{S}^1$ into six disjoint intervals of lengths $\frac{x_j}{2}, j = 1, 2, 3$ such that intervals of equal length are neighbouring. Then any map $T^{x_1,x_2,x_3} \in \mathrm{AR}(\mathbb{S}^1), (x_1, x_2, x_3) \in \Delta_2$ is a composition of two involutions: first, a simultaneous exchange of intervals of equal length and second, the rotation $R_{\frac{1}{2}}$. The family $\mathrm{AR}(\mathbb{S}^1)$ was first defined and studied by P. Arnoux and G. Rauzy in **[6]** and subsequently in **[3, 7, 9, 13]** and many other works.

Example. — A map $T^{\boldsymbol{a}} := T^{\boldsymbol{a},\boldsymbol{a}^2,\boldsymbol{a}^3}$ with $\boldsymbol{a} \in \mathbf{R}$ such that

$$\boldsymbol{a} + \boldsymbol{a}^2 + \boldsymbol{a}^3 = 1, \tag{4}$$

is called the **Arnoux-Yoccoz map**. It was first introduced and studied in **[8, 5]**. This map is the simplest minimal map in the family $\mathrm{AR}(\mathbb{S}^1)$, and has many autosimilarity properties.

The question of minimality in the Arnoux-Rauzy family has been explicitely solved by P. Arnoux and G. Rauzy in **[6]** where they have proven the following

Theorem 8. — **[6]** *A map in the Arnoux-Rauzy family is minimal, if and only if* $(x_1, x_2, x_3) \in \mathcal{R}$.

The proof by P. Arnoux and G. Rauzy is based on a process of renormalization which is defined as a first return map on the union of two intervals of continuity of the biggest (and equal) length. In this work we give a new proof of this theorem which is based on the following

Proposition 9. — **[25]** *The following sets of* 6*-IET on the unit circle coincide:*

$$\left\{T^{x_1,x_2,x_3} \in \mathrm{AR}(\mathbb{S}^1), (x_1, x_2, x_3) \in \Delta_2\right\} = \left\{F^2 \mid \ F^{l_1,l_2,l_3}_{\frac{1}{2}} \in \mathrm{CET}^3_{\frac{1}{2}}, (l_1, l_2, l_3) \in \Delta_2, \max(l_j) < \frac{1}{2}\right\}.$$

$$\textit{Moreover,} \quad l_j = \frac{1 - x_j}{2}, j \in \mathcal{N}_\Delta. \tag{5}$$

In this work we are interested in the dynamics of vertical foliations on a family of translation surfaces $X = X^{x_1,x_2,x_3}$ constructed as suspensions of maps $T = T^{x_1,x_2,x_3} \in \mathrm{AR}(\mathbb{S}^1)$ with $(x_1, x_2, x_3) \in \Delta_2$, as well of their real-rel leaves. For any translation surface X, one can consider local deformations of X in its stratum

in such a way that the singularities are moving one with respect to another while keeping the translational holonomies of closed curves on X fixed. This defines a **rel-foliation** in the stratum. The rel-foliations have been studied, among others, in **[39, 33, 24]** (under different terminologies). In the following we use the terminology from **[24]**.

Here we study the corresponding real-rel foliations constructed by variation of only horizontal holonomies on $X := X^{x_1,x_2,x_3}$. A surface X belongs to the stratum $\mathcal{H}(2,2)$, has genus 3 and two singularities. Hence for a fixed point $(x_1,x_2,x_3) \in \Delta_2$, its real-rel leaf $\{X_r\}$ is parametrized by one real parameter $r \in \mathbf{R}$. Here $X_0 = X$. By Proposition 9, the surface X_0 is a double cover of a non-orientable surface constructed as a suspension of a map in $\mathrm{CET}^3_{\frac{1}{2}}$. Hence, its real-rel deformation X_r naturally has its first-return map in CET^3_τ with τ and r connected by

$$r := \frac{1}{2} - \tau. \tag{6}$$

Moreover, the parameters (x_1,x_2,x_3) do not change on a real-rel leaf. This extends the equality in the Proposition 9 to, on the right, all of the maps in CET^3_τ and, on the left, the family of real-rel deformations of Arnoux-Rauzy maps.

6.3. Arithmetic orbits of real-rel leaves and billiard trajectories. — For the following study of the family CET^3_τ with $\tau \in \mathbb{S}^1$ we suppose, without loss of generality, $\tau \in [0,1/2]$. Indeed, a map $F^+_\tau := F^{l_1,l_2,l_3}_\tau \in \mathrm{CET}^3_\tau$ is conjugated to a map $F^-_{1-\tau} := F^{l_3,l_2,l_1}_{1-\tau} \in \mathrm{CET}^3_\tau$ via a change of orientation, $F^+_\tau = i \circ F^-_{1-\tau} \circ i$. Here i is a global involution on $\mathbb{S}^1, i : p \mapsto 1-p$. In particular, this means that the maps in $\mathrm{CET}^3_{\frac{1}{2}}$ have extra symmetries and commute with a global involution as noticed in [paragraph 4.1, **[25]**].

Lemma 3. — *Take any triple $(x_1,x_2,x_3) \in \Delta_2 \setminus \partial\Delta_2$. Let $T := T^{x_1,x_2,x_3} \in \mathrm{AR}(\mathbb{S}^1)$ and $X := X^{x_1,x_2,x_3}$ an associated translation surface. Then for any $r \in \left[0, \frac{1}{2}\right]$ the following holds:*

1. *let T_r be a first-return map on a horizontal transversal of a vertical flow on X_r in a real-rel leaf of X. Then $T_r = F^2$ with $F = F^{l_1,l_2,l_3}_\tau \in \mathrm{CET}^3_\tau$ defined by (5) and (6);*
2. *for any point $p \in \mathbb{S}^1$ the **displacement** $T_r(p) - p$ belongs to a finite set $\{0, \pm l_j \mid j \in \mathcal{N}_\Delta\}$;*
3. *moreover, if $r \leq \min\{x_j\}^3_{j=1}$, then for any $p \in \mathbb{S}^1$, $T_r(p) - p \neq 0$ and the map $T_r : \mathbb{S}^1 \to \mathbb{S}^1$ is a 6-IET with the intervals of continuity $I^\pm_j$, $|I^\pm_j| = \frac{x_j}{2} \pm r, j \in \mathcal{N}_\Delta$.*

Proof. — For $r = 0$, the statement of this Lemma is equivalent of that of Proposition 9. Moreover, the point 1. follows from the discussion above, since X is a double-cover of a projective plance with a first-return map equal to $F^{l_1,l_2,l_3}_{1/2}$.

Suppose now that $r \in \left(0, \min_j \left\{\frac{x_j}{2}\right\}\right)$ or, equivalently, $1/2 > \tau > \max(l_j)$. By a direct calculation, the map F^2 has 6 intervals of continuity:

$$\begin{aligned} I^+_2 := (l_2+\tau, 1)\,, I^-_2 := (0, \tau - l_2)\,, \\ I^+_3 := (\tau - l_2, l_1)\,, I^-_3 := (l_1, l_1 + \tau - l_3)\,, \\ I^+_1 := (l_1 + \tau - l_3, l_1 + l_2)\,, I^-_1 := (l_1 + l_2, l_2 + \tau)\,. \end{aligned}$$

The lengths of these intervals verify $|I^\pm_j| = \frac{x_j}{2} \pm r$. Then one has

$$I_1 = I^-_2 \cup I^+_3, \quad I_2 = I^-_3 \cup I^+_1, \quad I_3 = I^-_1 \cup I^+_2, \tag{7}$$

for the intervals $I_j, j \in \mathcal{N}_\Delta$ of continuity of F. The map F is an orientation reversing isometry on each of the intervals $I^\pm_j, j \in \mathcal{N}_\Delta$ and for any couple (j,k), with $j \neq k$, $|I^+_j| + |I^-_k| = (x_j + x_k)/2 = |I^-_j| + |I^+_k|$. This implies that the previous decomposition can be rewritten as

$$I_1 = F(I^-_3) \cup F(I^+_2), \quad I_2 = F(I^-_1) \cup F(I^+_3), \quad I_3 = F(I^-_2) \cup F(I^+_1),$$

and this decomposition is written with respect to the order on the circle. Then, one concludes by applying F one more time that the map $T = F^2$ maps the intervals $I^\pm_j$ onto the circle in a way that the intervals of the same index map to the neighbouring intervals but change the respective order.

The intervals $I^\pm_j$ can be distinguished by their symbolic dynamics, e.g. $I^+_1 = \{p \in \mathbb{S}^1 : p \in I_2, F(p) \in I_3\}$. Analogically, the first steps of accelerated symbolic codes of $I^-_1, I^+_2, I^-_2, I^+_3, I^-_3$ are cb, ca, ac, ab and ba correspondingly. The displacement for every $p \in I^\pm_j, j \in \mathcal{N}_\Delta$ can be calculated explicitely by the use of these codes. The displacement is equal to zero if and only if F has a 2-periodic interval (this happens if and only if $\tau \leq \max(l_j)$). □

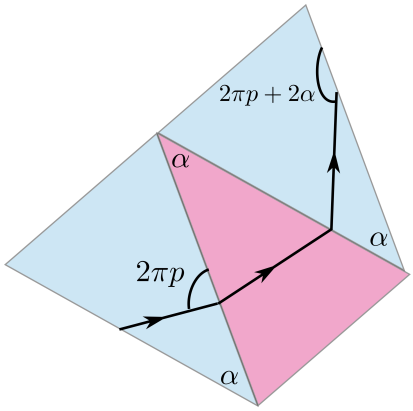

FIGURE 14. For a trajectory of angle $2\pi p$ with respect to a fixed line, after two reflections with respect to the sides c and b, this angle changes to $2\pi p + 2\alpha = 2\pi(p + l_1)$.

Remark 2. — From the point of view of triangle tiling billiards, the inclusion $T_r(p) - p \in \{\pm l_j\}$ represents a change of the direction of a trajectory after two refractions, see Figure 14 and [Theorem 3.6, **[12]**]. If the displacement for a map $F \in \mathrm{CET}^3_\tau$ is equal to 0, there is no corresponding billiard trajectory. The six-element set $\{\pm l_j\}$ has also been considered in relation to the artihmetic orbits of Arnoux-Rauzy maps by P. Hopper and B. Weiss in **[24]**, see their Proposition 4.6. The set of displacement values of T_r doesn't depend on r.

We now define the arithmetic orbits of the family of squares of the maps in the family CET^3_τ, here we follow **[24]**. For any map $F = F^{l_1,l_2,l_3}_\tau \in \mathrm{CET}^3_\tau$, let $T := F^2$. Let H be a group of rotations of $\mathbb{S}^1 = \mathbf{R}/\mathbb{Z}$ generated by six numbers $\pm l_j, j \in \mathcal{N}_\Delta$. Denote Γ the Cayley graph of H with respect to these six generators. Consider a periodic triangle tiling with the angles of tiles defined by the relation (2). We embed Γ to the plane to be the set of edges connecting the barycenters of all *positively oriented* triangles in this tiling. A point $p \in \mathbb{S}^1$ defines an embedded curve in the graph Γ, i.e. a sequence of elements $h_n \in H$ such that $T^n(p) - p = h_n \mod \mathbb{Z}$. We call $\{h_n\}$ the **arithmetic orbit** of p.

On a corresponding triangle tiling billiard the piece-wise linear curve $\gamma(p)$ (p and τ here define the initial conditions of the trajectory) starting in a *barycenter* of θ_0, and visiting the barycenters of the crossed tiles of the same orientation, coincides with the arithmetic orbit of p. This implies that the study of arithmetic orbits of the Arnoux-Rauzy maps and their real-rel deformations is equivalent to the study of triangle tiling billiard trajectories which are finer objects since they make two steps when an arithmetic orbit makes only one.

Note. — For all of the maps $T = F^2$ with $F \in \mathrm{CET}^3_\tau$ their SAF invariant (see **[5]** for definition) is zero. More generally, a square of any fully flipped IET has a zero SAF invariant. This statement has already been proven in **[25]** but we now give a simpler proof which is a remark by Victor Kleptsyn. A fully flipped map $F : \mathbb{S}^1 \to \mathbb{S}^1$ can be represented as a composition $F = i \circ H$ with $H \in \mathrm{IET}(\mathbb{S}^1)$ and i the global involution on $\mathbb{S}^1$. Obviously, $SAF(i \circ H \circ i) = -SAF(H)$. Since $SAF : \mathrm{IET} \to \mathbf{R} \wedge_{\mathbf{Q}} \mathbf{R}$ is a group homomorphism, we have: $SAF(F^2) = SAF(i \circ H \circ i \circ H) = SAF(i \circ H \circ i) + SAF(H) = -SAF(H) + SAF(H) = 0$.

7. Renormalization

A goal of this Section is to describe a renormalization process on the family CET^3_τ.

7.1. Complete periodicity and integrability.

— First,we deal with several simple cases.

For any map $F \in \mathrm{CET}^3_\tau$ we say that an interval $I \subset \mathbb{S}^1$ is **k-periodic** if $F^k \mid_I = \mathrm{id}$ for some $k \in \mathbf{N}^*$ (and such k is minimal). We call the set $\mathcal{P}_F$ of all $k \in \mathbf{N}^*$ such that there exists a k-periodic interval, the **set of interval periods** of the map F.

Lemma 4. — *Fix $(l_1, l_2, l_3) \in \Delta_2$ and $\tau \in [0, \frac{1}{2}]$. Then, the following holds for $F = F^{l_1,l_2,l_3}_\tau \in \mathrm{CET}^3_\tau$:*

1. *if $\tau \leq \max(l_j)$ then F is completely periodic. Moreover, if $\tau \in (0, \min(l_j)]$ then $\mathcal{P}_F = \{2, 6\}$. If $\tau \in (\min(l_j), \mathrm{mid}(l_j)]$ then $\mathcal{P}_F = \{2, 4n + 2, 4n + 6\}$, where $n = \lfloor \frac{\tau}{\min(l_j)} \rfloor \in \mathbf{N}^*$. In particular, if $l_j > \frac{1}{2}$ for some j, and $\tau \leq 1 - l_j$ then F is completely periodic;*
2. *if $l_j > \frac{1}{2}$ for some j, and $\tau > 1 - l_j$, then for any point $p \in \mathbb{S}^1$ either $F^2(p) = p$ or $F^2(p) = R_\kappa$ where R_κ is a rotation by $\kappa = \frac{l_3}{l_2 + l_3}$, defined on an entire interval I (with its endpoints identigied). This interval is defined as a connected component of points q such that $F^2(q) \neq q$, containing p;*

3. *the set $\mathcal{P}_F$ is finite in any of these cases, and $\mathcal{P}_F \subset \{4n+2 \mid n \in \mathbf{N}^*\}$ for point 1. and in point 2. it is as well if $\varkappa \notin \mathbf{Q}$.*

Proof. — We suppose that $l_1 \geq l_2 \geq l_3$. Define for any $j \in \mathcal{N}_\Delta$ the sets

$$K_j := I_j \cap F(I_j). \tag{8}$$

If $\tau \leq l_3$, then $F^2 \mid_{\cup_j K_j} = \mathrm{id}$ and the complement splits into 3 intervals in the same 6-orbit.

Second, if $\tau \in (l_3, l_2]$, then F has two 2-periodic intervals K_1 and K_2. Denote $I_1^- := (0, l_3), I_1^+ := (l_3, \tau), I_2^- := (l_1, l_1+\tau-l_3), I_2^+ := (l_1+\tau-l_3, l_1+\tau)$. Then $[0,1] = I_1^- \sqcup I_1^+ \sqcup K_1 \sqcup I_2^- \sqcup I_2^+ \sqcup K_2 \sqcup I_3$ and we have a following chain of images:

$$(0, l_3) = I_1^- \overset{F}{\longmapsto} I_2^+ \mapsto I_3 \overset{F}{\longmapsto} (\tau - l_3, \tau) \subset (0, \tau);$$
$$(l_3, \tau) = I_1^+ \overset{F}{\longmapsto} I_2^+ \overset{F}{\longmapsto} (0, \tau - l_3) \subset (0, \tau).$$

Then in restriction to $(0,\tau)$ the first return map F' of F is a 2-interval exchange transformation with combinatorics $\begin{pmatrix} \overline{I_1^-} & I_1^+ \\ I_1^+ & \overline{I_1^-} \end{pmatrix}$, where the flopped intervals are marked with bars, see **[25]** for more details on the notation. By **[27]**, such map is completely periodic, with $\mathcal{P}_{F'} = \{2n, 2n+2\}$, where $\frac{|I_1^-|}{|I_1^-|+|I_1^+|} = \frac{l_3}{\tau} \in [\frac{1}{n+1}, \frac{1}{n})$. This gives $\mathcal{P}_F = \{4n+2, 4n+6\}$.

Finally, suppose $\tau \in (l_2, l_1]$, then K_1 is the only 2-periodic interval for F. Consider now a subdivision: $I_1 = I_1^- \cup I_1^0 \cup I_1^+ \cup K_1, I_2 = I_2^- \cup I_2^+, I_3 = I_3^- \cup I_3^+$, with

$$I_1^- := (0, \tau - l_2), I_1^0 := (\tau - l_2, l_3), I_1^+ := (l_3, \tau)$$
$$I_2^- := (l_1, \tau + l_1 - l_3), I_2^+ := (\tau + l_1 - l_3, l_1 + l_2)$$
$$I_3^- := (l_1 + l_2, l_1 + \tau), I_3^- := (l_1 + \tau, 1).$$

Then we have a following chain of images:

$$I_1^- \overset{F}{\longmapsto} I_3^+ \overset{F}{\longmapsto} (l_2, \tau) \subset (0, \tau)$$
$$I_1^0 \overset{F}{\longmapsto} I_2^+ \overset{F}{\longmapsto} I_3^+ \overset{F}{\longmapsto} (\tau - l_3, l_2) \subset (0, \tau)$$
$$I_1^+ \overset{F}{\longmapsto} I_2^- \overset{F}{\longmapsto} (0, \tau - l_3) \subset (0, \tau).$$

This gives that the first-return map on $(0,\tau)$ has the combinatorics $\begin{pmatrix} I_1^- & \overline{I_1^0} & I_1^+ \\ I_1^+ & \overline{I_1^0} & I_1^- \end{pmatrix}$, with the lengths of its intervals of continuity $|I_1^-| = \tau - l_2, |I_1^0| = l_2 + l_3 - \tau, |I_1^+| = \tau - l_3$. This first return map is completely periodic since the Nogueira-Rauzy induction (see **[34, 25]** for more details) for this map stops, and its Rauzy diagram is finite. Indeed, one has a following Rauzy diagram:

$$\begin{pmatrix} I_1^- & \overline{I_1^0} & I_1^+ \\ I_1^+ & \overline{I_1^0} & I_1^- \end{pmatrix} \underset{|I_1^-|>|I_1^+|}{\overset{|I_1^+|>|I_1^-|}{\rightleftarrows}} \begin{pmatrix} I_1^- & \overline{I_1^0} & I_1^+ \\ I_1^+ & I_1^- & \overline{I_1^0} \end{pmatrix} \overset{|I_1^0|>|I_1^+|}{\to} \begin{pmatrix} I_1^- & \overline{I_1^+} & \overline{I_1^0} \\ I_1^+ & I_1^- & \overline{I_1^0} \end{pmatrix} \overset{|I_1^+|>|I_1^-|}{\to} \begin{pmatrix} \overline{I_1^-} & \overline{I_1^+} & \overline{I_1^0} \\ \overline{I_1^-} & I_1^+ & I_1^0 \end{pmatrix}. \tag{9}$$

We do not give a full Rauzy diagram but only one of its parts, since the diagram is symmetric with respect to the exchange of I_1^- and I_1^+. After a finite number of steps of the Rauzy-Nogueira induction, one obtains a completely periodic map (indeed, a permutation on the right in (9) is completely periodic). This proves the point 1.

For the point 2., if $l_1 > \frac{1}{2}$ and $\tau > 1 - l_1$ then we have $0 < l_1 + \tau - 1 < \tau < l_1$. Then the map F has two 2-periodic intervals $I_1^- := (0, l_1 + \tau - 1)$ and $I_1^+ := (\tau, l_1)$, $I_1^- \cup I_1^+ = K_1$. The first return map F^2 on the interval $I_2 \cup I_3 = (l_1, 1)$ coincides with a rotation R_κ with with $\kappa = \frac{l_3}{l_2+l_3}$.

Finally, for all the maps studied above the elements of $\mathcal{P}_F$ have the form $\{4n+2 \mid n \in \mathbf{N}\}$ (except for the point 2. and $\kappa \in \mathbf{Q}$ that may induce periods of the form $4n, n \in \mathbf{N}$). The set $\mathcal{P}_F$ is always finite. □

Remark 3. — In terms of triangle tiling billiards, the maps from Lemma 4 are **integrable**, i.e. the corresponding trajectories are either periodic (correspond to periodic intervals of period different from 2) or linearly escaping (correspond to the intervals of rotation in point 2. of the Lemma 4). The point 2. characterizes the linear escape on the obtuse triangle tilings. The point 1. corresponds to the trajectories that start far enough from the circumcenter and are periodic. For more on the integrability for tiling billiards, see [Section 5, **[25]**].

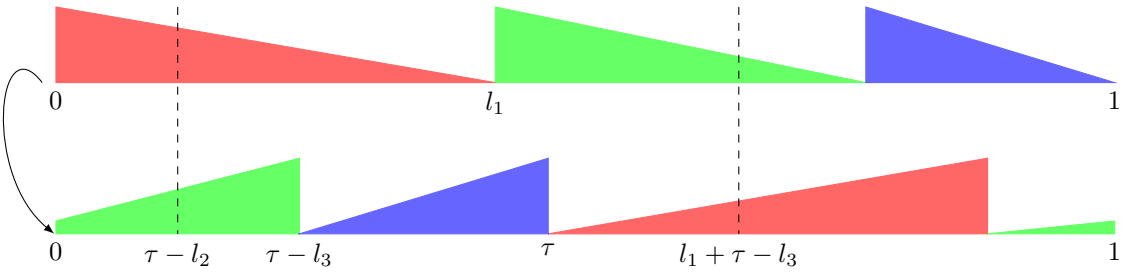

FIGURE 15. *Interval S_3 of the induction.* Here $F = F_\tau^{l_1,l_2,l_3} \in \mathrm{CET}_\tau^3$ with the parameters satisfying the relations $l_3 < l_2 \le l_1$ and $\tau \in \left(l_1, \frac{1}{2}\right]$. One step of renormalization gives a map R_3F which is a rescaled first return map on the interval S_3. The middlepoint of S_3 is equal to $\tau + l_1 - \frac{1}{2}$ and coincides with a singularity l_1 and only if $\tau = \frac{1}{2}$.

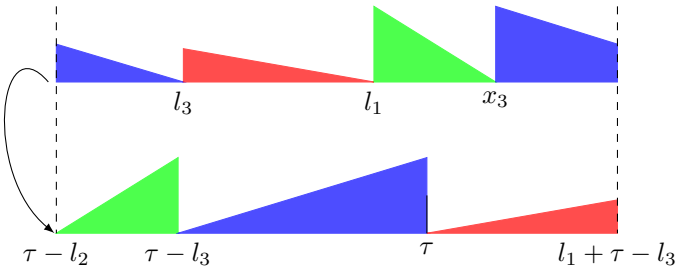

FIGURE 16. *First return map on S_3 is a fully flipped interval exchange transformation* with dynamics defined by(10) and (11). By regluing the extremities of S_3, a singularity between J_c^1 and J_c^2 dissapears.

7.2. Renormalization process. — Now we are ready to define the renormalization process on the family CET_τ^3: we will do it for all the cases that were not covered by the Lemma 4.

Theorem 9. — *Take a map $F = F_\tau^{l_1,l_2,l_3} \in \mathrm{CET}_\tau^3$ with $\tau \in [0, \frac{1}{2}]$. Let $\max\{l_j\}_{j=1}^3 \le \frac{1}{2}$ and $\tau > \max\{l_j\}_{j=1}^3$. Define x_j and r via the relations* (5) *and* (6)*. Then the following holds.*

1. *A map $T = F^2 : \mathbb{S}^1 \to \mathbb{S}^1$ is a 6-IET with intervals of continuity $I_j^\pm$ of lengths $|I_j^\pm| = \frac{x_j}{2} \pm r, j \in \mathcal{N}_\Delta$. Moreover, I_j^+ and I_j^- are neigbouring in the preimage, and their images $T(I_j^+)$ and $T(I_j^-)$ are neighbouring in the image.*
2. *Suppose that $l_j = \min\{l_j\}_{j=1}^3$ for some $j \in \mathcal{N}_\Delta$. Consider the interval $S_j := I_j^+ \cup I_j^- =: (s_j^-, s_j^+)$ and reglue its endpoints to obtain a circle $S_j/s_j^- \sim s_j^+$. Then a first return map on this circle is well-defined. Let $R_jF : \mathbb{S}^1 \to \mathbb{S}^1$ be its rescaling back to the unit circle. Then $R_jF \in \mathrm{CET}_\tau^3$ and its parameters $(l_1', l_2', l_3', \tau') \in \Delta_2 \times [0, 1/2]$ are defined as follows: (l_1', l_2', l_3') is th image of (l_1, l_2, l_3) under the fully subtractive algorithm, and*

$$\tau' = \frac{1}{2} - r', \quad r' = \frac{r}{|S_3|} \ge r.$$

3. *A map R_jF has a 2-periodic interval if and only if $l_j \ge \frac{1}{4} - \frac{r}{2}$.*

We call the interval I_j ***the interval in play****.*

Proof. — The point 1. follows from the proof of Lemma 3. As already mentionned before, the inequality $\tau > l_j$ is equivalent to the absence of 2-periodic intervals for F.

In the following we suppose that $l_3 = \min\{l_j\}_{j=1}^3$ or, equivalently, $x_3 = \max\{x_j\}_{j=1}^3$. Then $S_3 = (\tau - l_2, l_1 + \tau - l_3)$ and we study the first return map on S_3, see Figure 15.

Cut each of the intervals I_3^+ and I_3^- into two subintervals by points l_3 and x_3 correspondingly. Then $I_3^+ = J_3^2 \cup J_1$ and $I_3^- = J_2 \cup J_3^1$, where the intervals J_1, J_2, J_3^1 and J_3^2 are defined by

$$J_3^1 := (l_1 + l_2 - l_3, l_1 - l_3 + \tau)\,, J_3^2 := (\tau - l_2, l_3)\,,$$
$$J_1 := (l_3, l_1)\,,$$
$$J_2 := (l_1, l_1 + l_2 - l_3)\,.$$

We see that $|J_1| = \frac{x_3 - x_1}{2} = l_1 - l_3, |J_2| = \frac{x_3 - x_2}{2} = l_2 - l_3$ and $|J_3^1| + |J_3^2| = \left(\frac{x_2}{2} - r\right) + \left(\frac{x_1}{2} + r\right) = l_3$. Moreover, the interval S_3 is cut into four disjoint intervals in the following order:

$$S_3 = J_3^2 \sqcup J_1 \sqcup J_2 \sqcup J_3^1. \tag{10}$$

One can easily see that $F(J_1) \cup F(J_2) \subset S_3$, and that $F(J_1)$ is put to the right end of S_3, and $F(J_2)$ is put to the left end of S_3 by the dynamics. For the intervals J_3^1 and J_3^2, one has the following chains of iterations:

$$J_3^1 \overset{F}{\mapsto} I_2^- \overset{F}{\mapsto} (l_1 + l_2, l_1 + \tau) \overset{F}{\mapsto} (l_2, \tau) \subset S_3,$$
$$J_3^2 \overset{F}{\mapsto} I_1^+ \overset{F}{\mapsto} (l_1 + \tau, 1) \overset{F}{\mapsto} (\tau - l_3, l_2) \subset S_3.$$

Hence the first return map on S_3 coincides with F^3 in restriction to $J_3^1 \cup J_3^2$, see Figure 16.

Finally, we conclude that the images of the four intervals J_1, J_2, J_3^1, J_3^2 under the first return map cover S_3 without intersection. Indeed, we have

$$S_3 = F(J_2) \sqcup F^3(J_3^2) \sqcup F^3(J_3^1) \sqcup F(J_1). \tag{11}$$

Hence after regluing the ends of S_3 together and rescaling, we obtain a map $R_3F \in \mathrm{CET}_\tau^3$ with three intervals of continuity: the (rescaled) intervals J_1, J_2 and $J_3 = J_3^1 \cup J_3^2$. The direct calculation shows that $\tau = \frac{\tau - l_3}{|S_3|}$. By writing out $\tau = \frac{l_1+l_2+l_3}{2} - r$ we conclude $\tau' = \frac{1}{2} - \frac{r}{|S_3|}$. Thus the point 2. is proven.

Since $\tau > l_j$,$F(J_2) \cap J_2 = \emptyset$ and $F(J_1) \cap J_1 = \emptyset$ since $\tau > l_j$. Finally, $F^3(J_3^1) \cap J_3^1 \neq \emptyset$ is equivalent to the inequality $l_1 + l_2 - l_3 \leq \tau \Leftrightarrow l_3 \geq \frac{1}{4} + \frac{r}{2}$. Analogously, $F^3(J_3^2) \cap J_3^2 \neq \emptyset$ is equivalent to the analogous inequality $\tau - l_3 \leq l_3 \Leftrightarrow l_3 \geq \frac{1}{4} - \frac{r}{2}$. By uniting these two inequalities, we finish the proof of point 3. □

We now define the **renormalization process on the family** CET_τ^3 as follows. Take any map $F \in \mathrm{CET}_\tau^3$ and let $k = 0$, $F_0 = F$. If the conditions of Theorem 9 do not hold (equivalently, conditions of Lemma 4 do hold) for it, we say that the **renormalization process stops for the map** F. If these conditions do hold, that defines the index $t_1 \in \mathcal{N}_\Delta$ of the interval in play and a map $R_{t_1}F \in \mathrm{CET}_\tau^3$. One continues by recurrence. On the k-th step of the renormalization process (it if is defined), one obtains a map $F_k \in \mathrm{CET}_\tau^3$ defined by

$$F_k = R_{t_k} \circ \ldots \circ R_{t_1} F. \tag{12}$$

Here $\{t_k\} \in \mathcal{N}_\Delta^{\mathbf{N}}$ is a sequence of indices corresponding to the intervals in play.

Let $\boldsymbol{\lambda} := (l_1, l_2, l_3, \tau) \in \Delta_2 \times [0, \frac{1}{2}]$ a vector of parameters for any map $F \in \mathrm{CET}_\tau^3$. Then we denote by $\{\boldsymbol{\lambda}^{(k)}\}_{k \in \mathbf{N}}$ a sequence of such vectors corresponding to the maps F_k. Here $\boldsymbol{\lambda}^{(k)} = (l_1^{(k)}, l_2^{(k)}, l_3^{(k)}, \tau^{(k)}) \in \Delta_2 \times [0, 1/2]$. The corresponding vectors (x_1, x_2, x_3, r) are also defined in an analogous manner via (5) and (6).

We denote by $S^{(k)} \subset \mathbb{S}^1$ a set of definition of F_k, considered as a subset of the initial circle $S^{(0)}$, for any $k \in \mathbf{N}^*$. Obviously, the lengths $S^{(k)}$ diminish along the renormalization process since $S^{(k)} \subset S^{(k-1)}$.

Remark 4. — From the proof of Theorem 9 follows that one step (for example, $F \mapsto R_3F$) of the renormalization process corresponds to one step of the fully subtractive algorithm:

$$\left[l_1^{(1)} : l_2^{(1)} : l_3^{(1)}\right] = [l_1 - l_3 : l_2 - l_3 : l_3]. \tag{13}$$

The renormalization process in itself does not depend on the parameter τ (although the moment it stops does depend on τ). In coordinates x_j, the map (13) is nothing else than the Rauzy subtractive algorithm.

The fully subtractive algoritm is defined for all triples of l_j. Hence the Rauzy subtractive algorithm can be expanded to any triple (x_1, x_2, x_3) with $x_j \in [-1, 1]$, not necessarily positive, and it always continues with the index j in play for $x_j = \max\{x_j\}_{j=1}^3$.

Define the simplex $\Delta_2^\pm$ as a convex hull of the points $(1, 1, -1), (1, -1, 1)$ and $(-1, 1, 1)$. Then the Rauzy gasket is a part of $\Delta_2^\pm$ on which the fully subtractive algorithm is chaotic, and it is the complement of the three basins of attraction. This idea has been formulated in [**7**] by P. Arnoux and S. Starosta, see in particular their Figure 10. In terms of triangle tiling billiards, the fully subtractive algorithm is a renormalization on tilings, sending one tiling to an *a priori* different one.

7.3. Minimality in the family CET_τ^3**.** — The goal of this paragraph is to give a new proof of

Theorem 10 **([25]).** — *A map $F_\tau^{l_1,l_2,l_3} \in \mathrm{CET}_\tau^3$ is minimal if and only if $\tau = \frac{1}{2}$ and $(x_1, x_2, x_3) \in \mathcal{R}$.*

Our initial proof of this result with P. Hubert was based first, on Theorem 8 by Arnoux-Rauzy and second on the explicit study of (big) Rauzy graphs of 4-IET with flips. Indeed, we have proven the existence of an invariant of these graphs that implied the hyperbolicity of the Rauzy-Nogueira induction in the neighbourhood of the repelling hyperplane $\{\tau = \frac{1}{2}\}$. Although, the standard Rauzy-Nogueira induction is not the most appropriate tool to study the families of fully flipped maps since already one step of this induction gets out of such family. The renormalization process we propose above gives a much smaller graph - one vertex.

Here is a standard

Lemma 5. — *Consider a map $F \in \mathrm{CET}^3_\tau$ and the renormalization process for this map. Then a map F is minimal if and only if the renormalization process is infinite, and* $\lim_{k\to\infty} |S^{(k)}| = 0$.

Now we are ready to prove Theorem 10.

Proof. — Take a map $F \in \mathrm{CET}^3_\tau$ with a vector $\boldsymbol{\lambda}$of parameters. If the renormalization process reaches the k-th step, then for the map $F_k \in \mathrm{CET}^3_\tau, k \in \mathbf{N}^*$ defined by (12) we have

$$\boldsymbol{\lambda}^{(k)} = A_{t_k}\boldsymbol{\lambda}^{(k-1)},$$

where $t_k \in \mathcal{N}_\Delta$ are the indices of intervals in play and the matrices $A_j, j \in \mathcal{N}_\Delta$ are defined explicitely by

$$A_1 := \begin{pmatrix} 1 & 0 & 0 & 0 \\ -1 & 1 & 0 & 0 \\ -1 & 0 & 1 & 0 \\ -1 & 0 & 0 & 1 \end{pmatrix}, \quad A_2 := \begin{pmatrix} 1 & -1 & 0 & 0 \\ 0 & 1 & 0 & 0 \\ 0 & -1 & 1 & 0 \\ 0 & -1 & 0 & 1 \end{pmatrix}, \quad A_3 := \begin{pmatrix} 1 & 0 & -1 & 0 \\ 0 & 1 & -1 & 0 \\ 0 & 0 & 1 & 0 \\ 0 & 0 & -1 & 1 \end{pmatrix}.$$

Define now $B_j := \left(A_j^{-1}\right)^T, j \in \mathcal{N}_\Delta$. Then

$$B_1 = \begin{pmatrix} 1 & 1 & 1 & 1 \\ 0 & 1 & 0 & 0 \\ 0 & 0 & 1 & 0 \\ 0 & 0 & 0 & 1 \end{pmatrix}, \quad B_2 = \begin{pmatrix} 1 & 0 & 0 & 0 \\ 1 & 1 & 1 & 1 \\ 0 & 0 & 1 & 0 \\ 0 & 0 & 0 & 1 \end{pmatrix}, \quad B_3 = \begin{pmatrix} 1 & 0 & 0 & 0 \\ 0 & 1 & -1 & 0 \\ 1 & 1 & 1 & 1 \\ 0 & 0 & 0 & 1 \end{pmatrix}.$$

A map $F \in \mathrm{CET}^3_{\frac{1}{2}}$ if and only if $(\boldsymbol{\lambda}, \boldsymbol{v}^\perp) = 0$ for $\boldsymbol{v}^\perp := (1, 1, 1, -2)$. Moreover, the vector $\boldsymbol{v}^\perp$ is invariant for all three matrices $B_j, j \in \mathcal{N}_\Delta$, i.e. $B_j\boldsymbol{v}^\perp = \boldsymbol{v}^\perp$. This implies that

$$\left(\boldsymbol{\lambda}^{(0)}, v^\perp\right) = \left(A_{t_1}^{-1} \cdot \ldots \cdot A_{t_k}^{-1}\boldsymbol{\lambda}^{(k)}, v^\perp\right) = \left(\boldsymbol{\lambda}^{(k)}, B_{t_k} \cdot \ldots B_{t_1}v^\perp\right) = \left(\boldsymbol{\lambda}^{(k)}, v^\perp\right) = \left|S^{(k)}\right| - 2\tau^{(k)}\left|S^{(k)}\right|.$$

This calculation gives that $\tau^{(k)} = 1/2 - \frac{\left(\boldsymbol{\lambda}^{(k)}, v^\perp\right)}{\left|S^{(k)}\right|}$. Then $r^{(k)} = \frac{r^{(0)}}{|S^{(k)}|}$. Suppose now that F is minimal. Hence necessarily by Lemma 4, all renormalized maps F_k satisfy the conditions of Theorem 9. Then, by Lemma 5, one obtains that if $\left(\boldsymbol{\lambda}^{(k)}, v^\perp\right) \neq 0$, then $r^{(k)}$ tends to $-\infty$ while $k \to \infty$ which is impossible since $r^{(k)} \in [0, \frac{1}{2}]$. Hence necessarily $\left(\boldsymbol{\lambda}^{(k)}, v^\perp\right) = 0$ and $\tau^{(0)} = \tau^{(k)} = \frac{1}{2}$. Then, for $F \in \mathrm{CET}^3_{\frac{1}{2}}$ to be minimal, by Theorem 9, for every $k \in \mathbf{N}^*$ the following inequality should hold:

$$l_{t_k}^{(k)} < \frac{1}{4} - \frac{r^{(k)}}{2}. \tag{14}$$

Since $r^{(k)} = 0$, this implies $l_{t_k}^{(k)} < \frac{1}{4}$ for all $k \in \mathbf{N}^*$. In terms of parameters x_{t_k} these are equivalent to $x_{t_k}^{(k)} > 1 - x_{t_k}^{(k)}$ which, by definition gives $(x_1, x_2, x_3) \in \mathcal{R}$.

To prove the inverse statement,one can directly reference Theorem 8 and Proposition 9. Or, alternatively, if $F \in \mathrm{CET}^3_{\frac{1}{2}}$ with the parameters $(x_1, x_2, x_3) \in \mathcal{R}$, then the renormalization is always defined and $\left|S^{(k)}\right| \to 0$. This implies the minimality by Lemma 5. □

8. Classification of dynamics of triangle tiling billiards

We use the renormalization process on the family CET^3_τ and tiling billiard foliations in order to completely describe the dynamics of triangle tiling billiards.

8.1. Symbolic dynamics of triangle tiling billiards. — Now we prove the points 4. and 5. of Theorem 1, and confirm a so-called $4n + 2$ Conjecture in **[12]**.

Proof. — For any periodic billiard trajectory, consider a corresponding map $F \in \mathrm{CET}^3_\tau$ and periodic interval I of F. The map F is not minimal, and hence, the renormalization process stops for F. Then, by Theorem 9 and Lemma 4, I is necessarily flipped on itself or is periodic under a rational rotation R_κ (point 2. in Lemma 4). In the latter case, a map F can be perturbed by a slight change of parameters $(l_1, l_2, l_3) \in \Delta_2$ in order for $\kappa = \frac{l_3}{l_2+l_3} \notin \mathbf{Q}$. Then, the corresponding periodic interval disappears which is not the case for periodic orbits of triangle tiling billiards, see point 3. in Theorem 1. Indeed, this second case defines drift-periodic orbits. Hence, I is flipped on itself after a certain (odd) number of iterations, which proves the statement. □

Now let us relate the symbolic dynamics of $F \in \mathrm{CET}^3_\tau$ with that of its renormalization $RF \in \mathrm{CET}^3_\tau$.

Proposition 10. — *Consider one step of the renormalization process on* CET^3_τ. *Then for any orbit of the induced map* $R_jF, j \in \mathcal{N}_\Delta$, *the symbolic code of a corresponding orbit of* F *is obtained via the substitution* σ_j, *where*

$$\sigma_1 : \begin{cases} a \mapsto bca, \text{ if a precedent symbol was not } b, \\ a \mapsto cba, \text{ if a precedent symbol was not } c, \\ b \mapsto b, \\ c \mapsto c. \end{cases};$$

$$\sigma_2 : \begin{cases} a \mapsto a, \\ b \mapsto acb, \text{ if a precedent symbol was not } a, \\ b \mapsto cab, \text{ if a precedent symbol was not } c, \\ c \mapsto c \end{cases}; \tag{15}$$

$$\sigma_3 : \begin{cases} a \mapsto a, \\ b \mapsto b, \\ c \mapsto bac, \text{ if a precedent symbol was not } b, \\ c \mapsto abc, \text{ if a precedent symbol was not } a. \end{cases}$$

Consequently, if F_k *is defined by* (12) *then the symbolic code of any orbit of* F *is deduced from a symbolic code of a corresponding orbit of* F_k *by applying to it a substitution* $\sigma_{t_1} \circ \dots \sigma_{t_k}$.

Proof. — The proof follows from the proof of Theorem 9 and uses its notations. Suppose that $j = 3$. Then any orbit of the map F passes by a Poincaré section S_3. Moreover, for any point $p \in J_1 \cup J_2$, its F- and R_3F-orbits coincide, hence $\sigma_3(a) = a, \sigma_3(b) = b$. Finally, $J_3^1 \subset I_2, F(J_3^1) \subset I_1, F^2(J_3^1) \subset I_3$ and $J_3^2 \subset I_1, F(J_3^2) \subset I_2, F^2(J_3^2) \subset I_3$. Since both J_3^1 and J_3^2 both have the symbolic code c, σ_3 is defined conditionally. □

8.2. Complete description of the dynamics of triangle tiling billiards. — Now we are ready to prove Theorem 4 which is a much stronger version of Theorem 2 proven in [**25**].

Proof. — First, via the relations (2) and (5), we have $\rho_\Delta = (x_1, x_2, x_3)$. We now study the dynamics of a subfamily of maps in CET^3_τ with fixed (x_1, x_2, x_3) and varying τ, which corresponds to the study of the dynamics of a tiling billiard on a fixed tiling. Take a map F in this family.

Step 1. If the renormalization process stops for F, then by Lemma 4, all the corresponding billiard trajectories are either periodic or linearly escaping. Indeed, we have that $\tau^{(k)} \leq \max\{l_j^{(k)}\}_{j=1}^3$ or $l_j^{(k)} > \frac{1}{2}$ for some $j \in \mathcal{N}_\Delta$. In both cases, the dynamics of the map F_k is integrable, and hence is that of F.

If $\rho_\Delta \notin \mathcal{R}$, the renormalization process will necessarily stop, see Theorem 10.

Step 2. Take $\rho_\Delta \notin \mathcal{R}$. The linearly escaping behaviour exists on a corresponding tiling if and only if for some $k \in \mathbf{N}^*$, the map F_k verifies the conditions of point 2. in Lemma 4. An additional calculation shows that it is indeed true for all $\rho_\Delta \in \mathcal{R} \setminus \mathcal{E}$. The argument goes as follows.

Suppose that there exists some $k \in \mathbf{N}^*$ such that $l_i^{(k+1)} \neq 0$ for all $i \in \mathcal{N}_\Delta$ and

$$l_j^{(k+1)} > \frac{1}{2}|S^{(k+1)}|, \quad \textit{and } \forall m < k \quad \max\{l_i^{(m)}\}_{i=1}^3 \in [0, \frac{1}{2}). \tag{16}$$

In the above relation, necessarily $j = t_k$. Indeed, since $\max\{l_j^{(k)}\}_{j=1}^3 < \frac{1}{2}$ for $j \neq t_k$, we have

$$l_j^{(k)} - l_{t_k}^{(k)} < \frac{1}{2}\left(1 - 2l_{t_k}^{(k)}\right)$$

which is equivalent to $l_j^{(k+1)} < \frac{1}{2}$. Although, it is possible that (16) holds for $j = t_k$. This condition can be rewritten as

$$l_{t_k}^{(k+1)} > \frac{1}{2}|S^{(k+1)}| \Longleftrightarrow l_{t_k}^{(k)} > \frac{1}{2}(|S^{(k)}| - 2l_{t_k}^{(k)}) \Longleftrightarrow l_{t_k}^{(k)} > \frac{1}{4}|S^{(k)}|. \tag{17}$$

But the last inequaity holds for all $\rho_\Delta \notin \mathcal{R}_\Delta$ for some $k \in \mathbf{N}^*$. This implies that if $l_i^{(k+1)} \neq 0$ for all $i \in \mathcal{N}_\Delta$ then the linearly escaping behavior does occur on the triangle tiling defined by ρ_Δ. Indeed, it suffices to take $\tau^{(k+1)} = \tau^{(0)} = \frac{1}{2}$, by Lemma 4.

The case which is left is to study is what happens if for some $i \neq t_k, l_i^{(k)} = l_{t_k}^{(k)}$ (and hence $l_i^{(k+1)} = 0$). First, $l_1^{(k)} = l_2^{(k)} = l_3^{(k)} = \frac{1}{3}$ is equivalent to $\rho \in \mathcal{E}$. Since the dynamics on the equilateral triangle tiling is 6-periodic, then for any $\rho_\Delta \in \mathcal{E}$, by Theorem 9, all of the tiling billiard trajectories on the tiling defined by ρ_Δ, are periodic.

Otherwise, if there exists only one $j \neq k$ such that of $l_j^{(k)} = l_{t_k}^{(k)}$ coincide, without loss of generality we can suppose $t_k = 3$ and $j = 2$. Then $l_3^{(k)} = l_2^{(k)} \in [\frac{1}{4}, \frac{1}{3})$ and $l_1^{(k)} \in (\frac{1}{3}, \frac{1}{2}]$. Take $\tau^{(0)} = \frac{1}{2}$, then $\tau^{(k)} = \frac{1}{2}$. Then a map F_k is explicitely verified to have two types of orbits: fully flipped intervals of periods 6 (corresponding to

periodic orbits) and a periodic interval of period 4 which corresponds to a periodic linear drift Our argument also shows that 4 is the shortest period of the drift behaviour in a triangle tiling billiard. This implies that F has necessarily drift periodic orbits.

Step 3. If $\rho_\Delta \in \mathcal{R}$ and $\tau \neq \frac{1}{2}$, all corresponding trajectories are periodic. Indeed, it follows from Lemma 4, since the renormalizaiton stops at some step $k \in \mathbf{N}^*$ with $\max\{l_j^{(k)}\} < \frac{1}{2}$. For $\tau = \frac{1}{2}$, F is minimal by Theorem 10, and the corresponding trajectories escape. The inverse is true as well: escaping trajectories exist only for $\tau = \frac{1}{2}$.

Step 4. Finally, as shown in **[12]**, drift-periodic behaviour only occurs if $(l_1, l_2, l_3) \in \mathbf{Q}^3$. This also follows obviously from renormalization. Moreover, the arguments above show that for any tiling such that $(l_1, l_2, l_3) \in \mathbf{Q}^3 \setminus \mathcal{E}$ the drift-periodic trajectories exist, and only for them.

Step 5. First, for a tiling with $\rho_\Delta \in \mathcal{R}$ the set $\{G_\Delta^\delta\}$ of trees bounded by periodic trajectories is countable. Indeed, the symbolic codes of periodic trajectories coincide with the set $\{\sigma_{t_1} \circ \ldots \circ \sigma_{t_k} abcabc\}_{k \in \mathbf{N}}$, by Proposition 10. Second, for a tiling with $\rho_\Delta \notin \mathcal{R}$, the number of possible periodic behaviours is finite. Indeed, it is obviously true for any $\rho_\Delta \in \mathcal{E}$ and for $\rho_\Delta \notin \mathcal{E}$, the renormalization process stops at some obtuse triangle tiling on the step k. On this tiling, realizable trajectories with $\tau \in (1 - \max\{l_j^{(k)}\}, \frac{1}{2}]$ linearly escape by Lemma 4. For the tiling obtained on the k step, and $\tau^{(k)} = 1 - \max\{l_j^{(k)}\}$, the periods of corresponding trajectories are bounded. All of the other combinatorial behaviors are obtained by contraction of flowers inside these trajectories, hence the set of these is finite. Finally, the statement about the symbolic dynamics of linear escaping trajectories follows directly from point 2. in Lemma 4 and Proposition 10. □

Example. The set $\mathcal{E}$ is a countable set of preimages of a point $[1 : 1 : 1] \in \Delta_2$ under the fully subtractive algorithm that defines all of the triangle tilings on which billiard trajectories are always periodic. For example, a point $[1 : 2 : 2]$ corresponds to a tiling by triangles with angles $36°, 72°, 72°$ and all billiard trajectories in it have periods 6 or 10. The question whether the equilateral triangle tiling is the only tiling permitting *only* periodic trajectories was initially asked by Serge Troubetzkoy. Theorem 4 gives a negative answer to it.

9. Arithmetic orbits of Arnoux-Rauzy surfaces and exceptional trajectories

We are especially interested in the real-rel deformations of *minimal* Arnoux-Rauzy maps and their symbolic dynamics. The arithmetic orbits of minimal Arnoux-Rauzy maps are in the direct correspondance with exceptional triangle tiling billiard trajectories , see paragraph 6.3.

9.1. Exceptional trajectories pass by all tiles. — We remind our reader that by definition, the **exceptional trajectories** are those that are defined in the triangle tilings with $\rho_\Delta \in \mathcal{R}$ and pass through the circumcenters of crossed tiles.

Theorem 11. — *For any exceptional triangle tiling billiard trajectory δ the following holds:*

1. *if δ doesn't pass by any vertex of a tiling, then it passes by the interiors of **all** tiles.*
2. *if δ passes by some vertex $v \in V$ (is a singular ray) there exist 5 additional singular rays in a corresponding flower such that the union of these six rays passes by **all** tiles, and this union doesn't pass by any other vertex.*

Proof. — First, for any $\rho_\Delta \in \mathcal{R}$, the corresponding triangles are acute. Consider a base tile θ_0 and the folding map $\mathcal{F} = \mathcal{F}(\theta_0)$. Let l be a chord in a bellow such that $\mathcal{F}(\delta) \subset l$.

Let δ be a non-singular trajectory, hence $l \cap \mathcal{F}(V) = \emptyset$. Suppose that δ doesn't pass by all of the tiles. Hence there exists some tile θ in a tiling and its edge e such that $\delta \cap \theta \neq \emptyset$ and $\delta \cap \theta^e = \emptyset$. Consider a leaf δ' of the parallel foliation $\mathcal{P}^\delta$ passing by a circumcenter of θ^e. Then $\delta' \neq \delta$ and $\delta \cap e = \delta' \cap e = \emptyset$.

Consider now two singular segments of the foliation $\mathcal{P}^\delta$ in the tiles θ and θ^e. One can easily see from the folding that these segments may pass by the *same* vertex $v \in e$. Then, the corresponding singular trajectories are periodic by Theorem 4 and have to coincide since δ and δ' escape. We denote a corresponding periodic petal by δ_{τ_1}, see Figure 17. Now consider a family $\{\delta_\tau\}_{\tau \in [\tau_1, 1/2]}$ of trajectories passing by θ, with $\delta_{\frac{1}{2}} = \delta$. Since δ and δ' are escaping and belong to the same foliation, the trajectory δ_τ is periodic and passes by θ^e for any $\tau \neq \frac{1}{2}$. Moreover, we see that $\Omega_{\delta_{\tau_-}} \subset \Omega_{\delta_{\tau_+}}$ for any $\tau_-, \tau_+ \in [\tau_1, 1/2]$ such that $\tau_- < \tau_+$.

Hence, by passing to the limit, the trajectories δ and δ' can be both approached by a subsequence in a set of nested trajectories $\{\delta_\tau\}$ with $\tau \to \frac{1}{2}$. Hence $\delta \cap \delta' \neq \emptyset$. If δ is non-singular, then $\delta = \delta'$ and $\delta = \lim_{\tau \to \frac{1}{2}} \delta_\tau$ and δ passes by all the triangles.

Otherwise, if $\delta \cap \delta' \neq \emptyset$ then necessarily $\delta \cap \delta' = \{v\}$ for $v \in V$, then δ and δ' are singular rays in some unbounded flower. Then the parallel foliaiton $\mathcal{P}^\delta$ has 6 singular rays going out in each of the tiles in Θ_v since

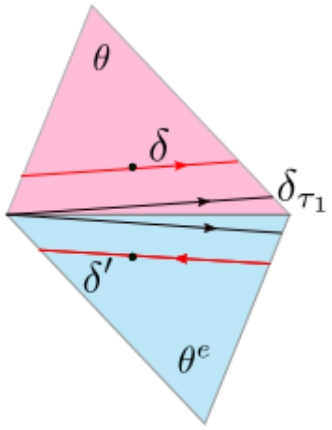

FIGURE 17. Two neighbouring tiles θ and θ^e and trajectories δ and δ' passing by circumcenters of the tiles. The trajectory δ_{τ_1} is a periodic loop containing e.

all the tiles are acute and the rays pass by a vertex and a circumcenter. Analogously to previous arguments, each of the sectors defined by these rays is foliated by sequences of periodic orbits with growing periods. Each ray separately spirals non-linearly to infinity.

Finally, a singular trajectory δ passing by a curcumcenter of a tile can't pass by two vertices of the tiling since there are no rational relationships between the angles of the tile with $\rho_\Delta \in \mathcal{R}$. □

Obviously, a trajectory passing by all points can't be linearly escaping. Hence the Theorem 11 implies that all of the exceptional trajectories (singular and non-singular) are non-linearly escaping which proves our conjecture with P. Hubert from **[25]**.

It can be interesting to study the growing fractal forms to which the exceptional trajectories converge after reparametrization and corresponding spanning trees. We do it in the following for the family of exceptional trajectories corresponding to the Arnoux-Yoccoz map.

9.2. A missing link: the Arnoux-Yoccoz map and the Rauzy fractal. — Consider the Arnoux-Yoccoz map $T^{\boldsymbol{a}} \in \mathrm{AR}(\mathbb{S}^1)$ defined in paragraph 6.2. By Lemma 3 and the vocabularly in the Table 1, we associate to it a map $F^{\boldsymbol{a}} \in \mathrm{CET}^3_{\frac{1}{2}}$ with its length parameters defined by

$$l_1 := \frac{1-\boldsymbol{a}}{2},\ \ l_2 := \frac{1-\boldsymbol{a}^2}{2},\ \ l_3 := \frac{1-\boldsymbol{a}^3}{2} \tag{18}$$

and a periodic triangle tiling with $\rho_\Delta = (\boldsymbol{a}, \boldsymbol{a}^2, \boldsymbol{a}^3)$ defined by (18) and its angles

$$\alpha = \frac{\pi}{2}(1-\boldsymbol{a}), \beta = \frac{\pi}{2}(1-\boldsymbol{a}^2), \gamma = \frac{\pi}{2}(1-\boldsymbol{a}^3). \tag{19}$$

A corresponding triangle is a **Tribonacci triangle** with $\alpha \approx 41°, \beta \approx 63°, \gamma \approx 76°$, and a corresponding billiard is the **Tribonacci billiard**. This billiard is the simplest one from all those that admit exceptional trajectories. The symbolic dynamics of these trajectories coincides with the arithmetic orbits of the Arnoux-Yoccoz map, see paragraph 6.3. Here we prove their convergence to the Rauzy fractal. We first remind some standard definitions.

A **Tribonacci substitution** σ_R acts on ${\mathcal{N}_\Delta}^{\mathbf{N}}$ and is defined as an extension of the map σ_R defined by

$$\sigma_R : \begin{cases} 1 \mapsto 12 \\ 2 \mapsto 13 \\ 3 \mapsto 1 \end{cases}.$$

The substitution σ_R has a unique fixed point $w_R \in {\mathcal{N}_\Delta}^{\mathbf{N}}$ which is a sequence of letters $w_{R,j} \in \mathcal{N}_\Delta, j \in \mathbf{N}$ and $w_R := 1213121121312\ldots$. We interpret the sequence w_R as an infinite ladder in the space $\mathbf{R}^3 =< e_1, e_2, e_3 >$ with standard cartesian coordinates and a standard basis. Each subsequent symbol $w_{R,j} \in \mathcal{N}_\Delta, j \in \mathbf{N}$ is interpreted as an addition of the step $e_{w_{R,j}}$ to the growing ladder. The infinite ladder constructed in this way has a principal direction. After projecting on a plane orthogonal to this direction, we consider the image of the set of endpoints. This set is, by definition, the **Rauzy fractal** and was defined by G. Rauzy in 1981, see **[35]**.

To a classic Tribonacci substitution σ_R one also associates a sequence of **Tribonacci numbers**, i.e. the sequence of lengths of iterations of the word 123 under the action of the substitution σ_R:

$$T_{n+4} := \left|\sigma_R^n(123)\right|, n \in \mathbf{N}. \tag{20}$$

We also set $T_1 = T_2 = T_3 := 1$. It is standard (and trivial) that for all n the following relation holds, generalizing the Fibonacci relation:

$$T_{n+3} = T_{n+2} + T_{n+1} + T_n, \tag{21}$$

which can also be seen as the definition. This sequence is the A000213 sequence of the on-line encyclopedia [**1**] of integer sequences [**1**].

The following is based on the fact that the point $\rho_\Delta = (\boldsymbol{a}, \boldsymbol{a}^2, \boldsymbol{a}^3) \in \Delta_2$ is a 3-periodic point of the Rauzy subtractive algorithm and equivalently, a triple (18) is a 3-periodic point of the fully subtractive algorithm. Indeed, we have $\left[\boldsymbol{a} : \boldsymbol{a}^2 : \boldsymbol{a}^3\right] \mapsto \left[\boldsymbol{a} - \boldsymbol{a}^2 - \boldsymbol{a}^3 : \boldsymbol{a}^2 : \boldsymbol{a}^3\right] = \left[\boldsymbol{a}^3, \boldsymbol{a}^2, \boldsymbol{a}\right]$. This implies that as an abstract tiling, the Tribonacci tiling is a fixed point of the renormalization. This also implies that the map $F^{\boldsymbol{a}}$ is a fixed point of the renormalization algorithm. Although, the map $R_1F^{\boldsymbol{a}}$ has the labels of its intervals of continuity changed. By Theorem 10, the map $F^{\boldsymbol{a}}$ is minimal hence all the corresponding exceptional trajectories are escaping, as already has been noticed in [**12**]. Moreover, by Proposition 10, the symbolic dynamics of its generic point is an invariant point of the substitution $\sigma := \sigma_1 \circ \sigma_2 \circ \sigma_3$ with σ_j defined explicitely by (15).

Define a following map $\upsilon_{\text{rel}} : \mathcal{A}_\Delta^{\mathbf{N}} \to \mathcal{A}_\Delta^{\mathbf{N}}$ by extending via concatenation the following map on the letters in $\mathcal{A}_\Delta$:

$$\upsilon_{\text{rel}} : \begin{cases} a \mapsto b, \\ b \mapsto c, \\ c \mapsto a, \end{cases} .$$

Now let $\varsigma_R := \upsilon_{\text{rel}} \circ \sigma_3$ be a substitution on cyclic periodic words in the alphabet $\mathcal{A}_\Delta$.

Since all the words in the orbit $\{\varsigma_R^j(cba)\}_j$ are symbolic codes of Tribonacci tiling billiard trajectories, they do not contain two equal letters subsequently and in restriction to this orbit, one can define ς_R as

$$\varsigma_R : \begin{cases} a \mapsto b \\ b \mapsto c \\ c \mapsto cba, \textit{if a precedent symbol is } a \\ c \mapsto bca, \textit{if a precedent symbol is } b \end{cases} . \tag{22}$$

We now define the **factorization map** υ_{fac} on the words in $\mathcal{A}_\Delta^2$ (or, equivalently, on the even-length words in $\mathcal{A}_\Delta$). Define $\upsilon_{\text{fac}} : \mathcal{A}_\Delta^2 \to \mathcal{N}_\Delta$ by extension of the map explicitely defined on the letters if $\mathcal{A}_\Delta^2$ by

$$\upsilon_{\text{fac}}(ab) = \upsilon_{\text{fac}}(ba) := 3,$$
$$\upsilon_{\text{fac}}(ac) = \upsilon_{\text{fac}}(ca) := 2,$$
$$\upsilon_{\text{fac}}(cb) = \upsilon_{\text{fac}}(cb) := 1.$$

Define for any map $\varphi : (\mathcal{A}_\Delta^2)^{\mathbf{N}} \to (\mathcal{A}_\Delta^2)^{\mathbf{N}}$ its **factorization** $\varphi^* : (\mathcal{N}_\Delta)^{\mathbf{N}} \to (\mathcal{N}_\Delta)^{\mathbf{N}}$ as the solution of the commutative relationship: $\upsilon_{\text{fac}} \circ \varphi = \varphi^* \circ \upsilon_{\text{fac}}$. The connection between σ_R and ς_R is now apparent through this factorization.

Proposition 11. — *The factorizations $\sigma_j^*, \upsilon_{\text{rel}}^*$ and ς_R^* of the substitutions $\sigma_j, j \in \mathcal{N}_\Delta$, υ_{rel} and ς_R are well defined. Moreover, even though the substitutions σ_j are defined only for cyclic words, their factorizations σ_j^* are well defined for string words. Finally, $\varsigma_R^* = \sigma_R$.*

Proof. — This is a simple verification. First, for the action of σ_1 on two-letter words, we have that $\sigma_1(ba) = bcba$ and

$$\sigma_1(ab) = \begin{cases} cbac \\ bcab \end{cases} .$$

These three equations factorize correctly into one equation $\sigma_1^*(3) = 13$ which proves that $\sigma_1^*(3)$ is well-defined.

Similarly, $\sigma_1(ac) = cbac$ or $bcac$ and $\sigma_1(ca) = cbca$ and $\sigma_1^*(2) = 12$ is well defined. The rest of verifications is done analogously and one obtains that the maps σ_j^* are well-defined on string words as extensions of the following substitutions:

$$\sigma_1^* : \begin{cases} 1 \mapsto 1 \\ 2 \mapsto 12 \\ 3 \mapsto 13 \end{cases} , \quad \sigma_2^* : \begin{cases} 1 \mapsto 21 \\ 2 \mapsto 2 \\ 3 \mapsto 23 \end{cases} , \quad \sigma_3^* : \begin{cases} 1 \mapsto 31 \\ 2 \mapsto 32 \\ 3 \mapsto 3 \end{cases} .$$

The factorization of the map $\upsilon_{\rm rel}$ is obviously given by $\upsilon^*_{\rm rel}(1) = 2, \upsilon^*_{\rm rel}(2) = 3, \upsilon^*_{\rm rel}(3) = 1$. The final calculation gives that $\varsigma^*_R = \upsilon^*_{\rm rel} \circ \sigma^*_3 = \sigma_R$. For $\sigma = (\sigma_1 \circ \sigma_2 \circ \sigma_3)$ we have $\sigma^* = \sigma^*_1 \circ \sigma^*_2 \circ \sigma^*_3 = \sigma^3_R$. □

Example. — The image of the cyclic periodic word *cbacba* by σ and a corresponding relabelled sequence $\{w_j\}$ with $w_j = \varsigma_R^{j-1}\left(\overline{cba}\right), j \in \mathbf{N}^*$, are calculated as follows:

$$w_1 = \overline{cba} \overset{\sigma_3}{\longmapsto} \overline{bacba} \overset{\sigma_2}{\longmapsto} \overline{cabacacba} \overset{\sigma_1}{\longmapsto} w_4 = \overline{cbcabcbacbcacbcba},$$
$$w_1 = \overline{cba} \overset{\varsigma_R}{\longmapsto} w_2 = \overline{cbacb} \overset{\varsigma_R}{\longmapsto} w_3 = \overline{bcacbcbac} \overset{\varsigma_R}{\longmapsto} w_4 = \overline{cbcabcbacbcacbcba}.$$

Since $\upsilon_{\rm fac}(cbacba) = 123$, then by Proposition 11, we have $\upsilon_{\rm fac}(w_j) = \sigma_R^{j-1}(123)$. As already noticed before, the words w_j describe the complete set of symbolic codes of periodic trajectories of the Tribonacci billiard.

Let us now make the emerging connection between the Tribonacci billiard and the Rauzy fractal precise.

Let us inroduce the following notations. We write $U_1 = U_2$ for two elements $U_1, U_2 \in \mathcal{A}^{\mathbf{N}}_\Delta$ if their corresponding cyclic words are equal and we write $U_1 \equiv U_2$ if these two elements coincide symbol by symbol as string words in $\mathcal{A}^{\mathbf{N}}_\Delta$.

We define a sequence of words $\{s_j\}_{j=-2}^{\infty}$, $s_j \in \mathcal{A}^{\mathbf{N}}_\Delta$ with $s_j \equiv s^1_j \dots s^{l_j}_j$, $s^i_j \in \mathcal{N}_\Delta$ and $l_j = |s_j| \in \mathbf{N}^*$ as follows. First let $s_{-2} :\equiv a, s_{-1} :\equiv b, s_0 :\equiv c, s_1 :\equiv cba$.

Then, for any $j \in \mathbf{N}^*$ we deduce the word s_{j+1} by recurrence from s_j. If $s^1_j \neq c$, let $s_{j+1} :\equiv \varsigma_R(s_j)$. Otherwise, if $s^1_j = c$, $s_j = c\, s^2_j \ \dots \ s^{l_j}_j$, we define the string s_{j+1} by

$$\varsigma_R(s_j) \equiv k^j_1\, k^j_2\, a\, \varsigma_R(s^2_j) \dots \varsigma_R(s^{l_j}_j) = a\, \varsigma R(s^2_j) \ \dots \varsigma_R(s^{l_j}_j)\, k^j_1\, k^j_2 \equiv: s_{j+1}.$$

Here $(k^j_1, k^j_2) = (b, c)$ if $s^{l_j}_j = b$ and $(k^j_1, k^j_2) = (c, b)$ if $s^{l_j}_j = a$. Of course, the equality of cyclic words $s_{j+1} = \varsigma_R(s_j)$ holds.

Define the cyclic words $w_j := s^2_j$. Obviously, as cyclic words, they are as above, the subsequent images of the word $\overline{cba}$ under the substitution ς_R. Denote $P_j := |w_j|$, i.e. $P_j = 2l_j$. We also define the word w_∞ as a fixed point of ς_R. In the following, we consider s_j as string words and w_j as cyclic words. The string words s_j here coincide with the symbolic codes of a singularity for the maps $F^{\boldsymbol{a}}_r$ in the family of real-lef deformations for the Arnoux-Yoccoz map $F^{\boldsymbol{a}}$, with the parameter $r \to 0$ as $j \to \infty$.

Example. — The next 4 elements of the sequence $\{s_j\}_{j \in \mathbf{N}^*}$ are

$$s_2 :\equiv acbcb,$$
$$s_3 :\equiv bcbacbcac,$$
$$s_4 :\equiv cbcacbcbacbcabcba,$$
$$s_5 :\equiv acbcabcbacbcacbcbacbcabcbcacbcb.$$

While interested in [**24**] in the dynamics of real-rel leafes of Arnoux-Yoccoz surfaces, P. Hooper and B. Weiss conjectured that the arithmetic orbits of the Arnoux-Yoccoz map $T^{\boldsymbol{a}}$ converge to the Rauzy fractal in the Hausdorff topology, up to rescaling and uniform affine coordinate change. Subsequently, P. Baird-Smith, D. Davis, E. Fromm and S. Iyer, following the connection between the arithmetic orbits and trajectories of tiling billiards they have discovered, restated the Hooper-Weiss Conjecture in terms of triangle tiling billiards. The following Theorem gives a proof of their conjecture by including all of the real-rel deformations of the Arnoux-Yoccoz surface in one dynamical system, the Tribonacci billiard.

For any word $w \in \mathcal{A}^{\mathbf{N}}_\Delta$, if this word finishes by a word $\varkappa$, we denote by $w^{\varkappa}$ the word such that $w = w^{\varkappa}\varkappa$.

Theorem 12 **(Combinatorics of Tribonacci billiards).** — *Consider the Tribonacci billiard and its trajectory δ_{AY} passing by a circumcenter of some tile. If δ_{AY} is not singular then the following holds:*

1. *all of the non-singular leaves in $\mathcal{P}^{\delta_{AY}}$, except for δ_{AY}, are periodic and δ_{AY} passes by all tiles,*
2. *for any $\delta \neq \delta_{AY}$ in $\mathcal{P}^{\delta_{AY}}$ (oriented counterclockwise), there exists $j \in \mathbf{N}^*$ such that its symbolic code is equal to $w_j = \varsigma_R^{j-1}(\overline{cba})$,$w_j = s^2_j$. The period of δ is then a doubled Tribonacci number $2T_{j+3}$. Moreover, $\upsilon_{\rm fac}(w_j) = \sigma_R^{j-1}(123)$ and $\upsilon_{\rm fac}(w_\infty) = w_R$,*
3. *any trajectory $\delta \in \mathcal{P}^{\delta_{AY}}$ with its symbolic code w_j defines a unique family $\Gamma_\delta = \{\gamma_k, k \in \mathbf{N}^*\}$ of flowers in $\mathcal{P}^{\delta_{AY}}$ (except for γ_2 which is not a flower but a petal of a two-petal flower γ_3) with pistils in vertices $v_k \in V$ (for $k = 2$, we define $v_2 = v_3$) that satisfy the following properties:*
   a. *if $j \geq 3$, the trajectory δ is contracted in the direction of its inside normal onto the flower γ_j, if $j = 1$ then δ contracts on $\gamma_0 = \{v_1\}$, if $j = 2$ it contracts on a one-petal flower γ_1,*
   b. *every $\gamma_k \in \Gamma, k \in \mathbf{N}^*$ passes by all of the the six tiles in Θ_{v_1},*

c. for all $k \in \mathbf{N}^*$, a flower (petal) γ_k has combinatorics w_k (i.e. there exists a periodic trajectory close to this flower with this combinatorics),

d. any γ_k with $k \geq 4$ is a flower with three petals,

4. the family Γ_δ has the following autosimilarity properties:

4.1 for any $k \geq 4$, a flower γ_k has three petals with combinatorics $w_{k-3}, w_{k-2}, w_{k-1}$, and is contained inside the biggest petal of the flower γ_{k+1}; a flower γ_3 has two petals of combinatorics w_2, w_1, a flower γ_1 also has one petal of combinatorics w_1,

4.2 the string symbolic words $s_k^2, j \in \mathbf{N} \cup \{-2, -1\}$ satisfy the following relationships, with $\varepsilon(k) := k \bmod 3$:

$$(s_{k-3} \cdot s_{k-3})^* \ \dagger \ (s_{k-2}^2)^\star \ * \ (s_{k-1}^2)^\dagger \star \equiv s_{k-3} \cdot ((s_k)^2)^{s_{k-3}} = s_k^2 = w_k, \tag{23}$$

where $(*, \star, \dagger) : \mathbf{N}^* \to \mathcal{A}_\Delta^3$ is defined explicitely by $(*, \star, \dagger) = (c, a, b)$ if $\varepsilon = 0$, $= (a, b, c)$ if $\varepsilon = 1$, $= (b, c, a)$ if $\varepsilon = 2$. Moreover, the edges corresponding to the symbols $\dagger, *$ and $\star$ in the representation (23) meet in v_k. On each new step of the construction, the pistil $v_{k+1} \in V$ is uniquely defined by first, $v_{k+1} \notin \Omega^{\gamma_k}$ and $v_{k+1} \in e_k$ where the edge e_k is crossed by the smallest of the three petals of the flower γ_k on the half of its length starting from v_k (in the symbolic code (23), it corresponds to the middlepoint $\cdot$ marked on the right-hand side),

5. for any flower $\gamma_k, k \geq 4$, we denote by $\Omega_k^1, \Omega_k^2, \Omega_k^3$ the unions of all the tiles by which pass its petals, in the order of decreasing period. Then for a matrix $A = \begin{pmatrix} -a & 1 \\ -1-a^2 & -1 \end{pmatrix}$ defined in **[35]** *one has (the two last lines, up to an isometry of the plane)*

$$\begin{aligned} \Omega_{k+1}^1 &= \Omega_k^1 \cup \Omega_k^2 \cup \Omega_k^3, \\ \Omega_{k+1}^2 &= A\Omega_k^1, \\ \Omega_{k+1}^3 &= A\Omega_k^2. \end{aligned}$$

This implies that the sequence of curves $A^{-k}\gamma_k$ approximates the Arnoux-Rauzy curve. Moreover, the sets of all barycenters of tiles in the partition $A^{-k}\Omega_{k+1}^1 = A^{-k}\Omega_k^1 \cup A^{-k}\Omega_k^2 \cup A^{-k}\Omega_k^3$ give a sequence of approximations of the Rauzy fractal. Finally, a sequence of curves $\{A^{-k}\delta_{AY}\}_{k \in \mathbf{N}^*}$ on the plane converges to the Arnoux-Rauzy curve, in restriction to the fundamental domain which is a limit set of the sets $A^{-k}\Omega_{k+1}$ in the Haudorff topology. The distance $d(\theta_n, \theta_0)$ between the triangle θ_n that δ_{AY} visits at its nth iteration and its initial triangle θ_0 verifies

$$d(\theta_n, \theta_0) \sim C \cdot \sqrt{n}, n \to \infty.$$

Finally, if δ_{AY} is singular (in some point $v \in V$) then the corresponding foliation $\mathcal{P}^{\delta_{AY}}$ has 5 additional singular rays entering the tiles in Θ_v. Each of the sectors defined by these rays is foliated by sequences of periodic orbits with growing periods that approach Rauzy fractal, up to the reparametrization described above.

Proof. — The renormalization process defined in the Part II applied to the Tribonacci tiling translates to a construction of a growing sequence of flowers in the foliation $\mathcal{P}^{\delta_{AY}}$, and completely describes its dynamics.

The point 1. has been already proven in Theorem 11. The point 2. follows from Theorem 9, Proposition 10 and Proposition 11.

By Theorem 6, the periodic trajectories on one side of δ_{AY} have the same winding. Fix a trajectory δ with symbolic dynamics w_j. In order to construct the family Γ_δ, we proceed as follows. We contract δ inside onto some flower, choose the biggest petal of this flower, and a periodic trajectory approaching this petal from inside, and repeat. Thus we construct a sequence of flowers γ_k with diminishing periods till $\gamma_0 := \{v_0\}$, with periods in the set of doubles Tribonacci numbers. It is known and easily proved that if $p \in \mathbf{N}^*, p \geq 8$ then p has a unique Tribonacci representation $p = \sum_i \varepsilon_i T_i$, where $\varepsilon_i = 0, 1$ and $\varepsilon_i \varepsilon_{i+1} \varepsilon_{i+2} = 0$ for all i. This implies that for $k \geq 4$, the petals of the flower γ_k with combinatorics w_k have combinatorics $w_{k-1}, w_{k-2}, w_{k-3}$ for all $k \geq 4$. The combinatorics of a sequence of flowers $\{\gamma_j\}$, with small indices (for $j \leq 4$), follows from explicit calculation, see Figure 18. By construction, all of the curves γ_k pass by the six tiles in Θ_{v_0}. This finishes the proof of point 3 and that of point 4.1.

The statement 4.2. is verified explicitely for all $k \leq 4$. Let us now explain this statement for any k, by reccurence. For the flower γ_k obviously, the word $s_{k-3} \cdot (s_k^2)^{s_{k-3}}$ coincides cyclically with w_k. The left-hand side of (23) coincides with w_k as well since a flower is a union of three petals, in the presented order. Indeed, the flower γ_{k-1} is mapped to γ_k va renormalization and the pistil v_k is mapped to the pistil v_{k+1}. The junctions $*, \star, \dagger$ in γ_k hence correspond to the three edges that are crossed by a close periodic trajectory (and not contained in the flower itself). These are three edges such that $* \cap \star \cap \dagger = \{v_k\}$. The vertices $\{v_k\}$ are related to the

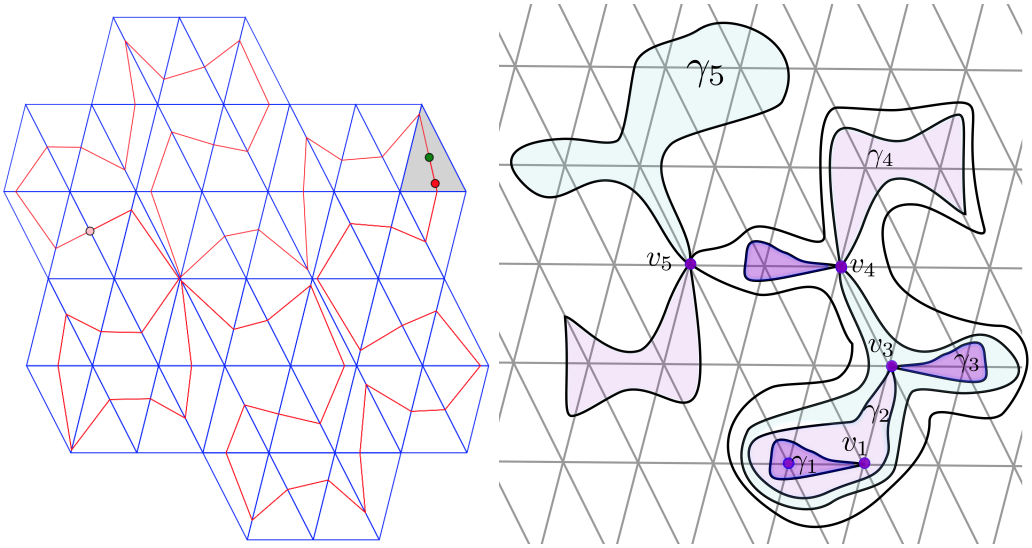

FIGURE 18. *Flowers in the foliation* $\mathcal{P}^{\delta_{AY}}$. On the left, a periodic trajectory δ of period $62 = 2 \cdot 31$. On the right, the subset $\{\gamma_k\}_{k=1}^5$ of the set Γ_δ of flowers defined by δ. The zones of equal symbolic behavior in $\mathcal{P}^{\delta_{AY}}$ have the same color. On the right, we do not draw the exact trajectories but curves with equal symbolic codes.

symbolic dynamics in a following way. For any k there exists a unique edge e_k which is crossed by a smallest petal of γ_k in the middle of its symbolic dynamics (starting from the vertex v_k). The vertex of this edge contained outside Ω^{γ_k} is exactly v_{k+1}, via renormalization.

The relationships between the sets Ω_k^j follow obviously from above. Moreover, since the square of the renormalization is the Rauzy substitution, the reparametrization matrix is the same as that in **[35]**. All of the rest follows from standard results and arguments.

The difference between the non-singular and singular cases, is that in the first case δ_{AY} passes by all triangles in the tiling. In the second case, is is stopped in a vertex (which coincides with some v_k defined above). The rest of the argument follows from the arguments in Theorem 11. □

9.3. Other fractal curves. — In addition to its arithmetic orbits, a few other fractal objects may be associated to the Arnoux-Yoccoz map. Initially, P. Arnoux in **[4]** constructed a semi-conjugacy h between the map $T^{\boldsymbol{a}}$ and a translation $T_{\mathbb{T}}$ on the torus with a translation verctor equal to $(\boldsymbol{a}, \boldsymbol{a}^2)$. A curve defined as $h(\mathbb{S}^1)$ is a **Peano curve on the torus** which can be approximated by a sequence of piecewise linear curves, since the map h maps the $(T^{\boldsymbol{a}})^k(\frac{1}{2})$ to $T_{\mathbb{T}}^k(0)$ for all $k \in \mathbf{N}$.

Following the works **[32]** and **[29]**, we define an **algebraic fractal curve** associated to the map $T^{\boldsymbol{a}}$. For any $p \in \mathbf{Q}[\boldsymbol{a}, \boldsymbol{a}^2] =< 1, \boldsymbol{a}, \boldsymbol{a}^2 >$ its image $T^{\boldsymbol{a}}(p) \in \mathbf{Q}[\boldsymbol{a}, \boldsymbol{a}^2]$. For any point p one draws a piece-wise linear curve connecting the subsequent points in its orbit in the 3-dimensional vector space $\mathbf{Q}[\boldsymbol{a}, \boldsymbol{a}^2]$. Such a curve is contained between two parallel planes. By projecting it on one of these planes, for a typical point $p \in \mathbf{Q}[\boldsymbol{a}, \boldsymbol{a}^2]$, one obtains a fractal curve, see **[32]** for more details and a picture. In **[29]**, J. Lowenstein, F. Poggiaspala and F. Vivaldi study the density properties of such a curve. It is interesting to compare their results with our Theorem 11.

The algebraic fractal curve, the Peano curve on the torus, as well as the Rauzy fractal, all converge one to another up to resclaing, as proven in **[3]**. From our Theorem 12 follows that the arithmetic orbits of the Arnoux-Yoccoz map can be joined to this list of curves, thus proving that all of the fractal curves associated to the Arnoux-Yoccoz map, up to reparametrization, represent the same object. We also believe that it is interesting to include the objects constructed by T. Coulbois and M. Minervino **[15]** in this list. We hope that our results may permit to reinforce the results in **[29]**, find simple proofs of the results in **[3]** and in general, clarify the connections between all of these beautiful fractal objects.

Theorem 12 can be generalized in order to prove the results on the convergence of other exceptional trajectories to fractals (and hence, arithmetic orbits of other minimal maps in the Arnoux-Rauzy family), at least for the periodic points of the Rauzy subtractive algorithm. It is an interesting question to study such convergence for all $\rho_\Delta \in \mathcal{R}$. At least two interesting questions follow. First, what fractal curves arise as arithmetic orbits? And second, what are possible dilatation coefficients of corresponding pseudo-Anosov maps?

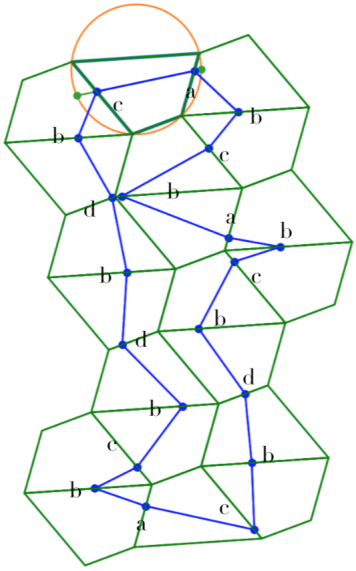

FIGURE 19. Quadrilateral billiard trajectory with a symbolic code $w = cabcbabcbdbcabcbdbdb$.

PART III. GENERALIZATIONS AND OPEN QUESTIONS

10. Dynamics of quadrilateral triangle tiling billiards

The theory of tiling billiards in cyclic quadrilateral tilings is in many ways analogous to that of triangle tiling billiards since a folding map into a disk is well defined as well as tiling billiard foliations. Moreover, the connection with a family of fully flipped maps on the circle persists. Although, the renormalization process we define for CET^3_τ doesn't seem to extend in a straightforward way to the family CET^4_τ. In this Section, we discuss the challenges and open questions.

10.1. Tree conjecture for quadrilateral tiling billiards. — Analogously to the case of triangle tilings, we define the graphs $\Lambda_\square$ and $G^\delta_\square$ and we formulate

***Conjecture 1* (Tree conjecture for cyclic quadrilateral tilings).** — *Take any periodic trajectory δ of a cyclic quadrilateral billiard. Then the set $G^\delta_\square := \Omega^\delta \cap \Lambda_\square$ is a* tree *(as a subgraph of $\Lambda_\square$).*

By Proposition 2, it is sufficient to prove the Bounded Flower Conjecture for cyclic quadrilateral tilings. Even though one can prove easily the analogue of Proposition 1, the global symbolic behavior of quadrilateral tiling billiards is more complicated than that of triangle tilings. The trajectories in quadrilateral tilings are not symmetric, e.g. their symbolic codes do not necessarily belong to the set $\{4n+2, n \in \mathbf{N}^*\}$ since already on the square tilings there exist 4-periodic orbits. This is far to be an only example: there exist highly asymmetric trajectories, see Figure 19.

We suspect that the analogue of the renormalization process can be defined for CET^4_τ. This process should correspond to the contraction of flowers in the parallel foliation, or in other words, to the contraction of leaves of measured foliations on the projective plane onto traintracks. We hope to explore this idea in our future work.

10.2. Density property for triangle and quadrilateral tiling billiards. — The behavior of periodic trajectories expressed in Theorem 3 can be generalized to escaping trajectories that *dynamically construct* two graphs, both of which are trees.

Consider a (not necessarily periodic) trajectory δ in a triangle (or cyclic quadrilateral) tiling billiard. Define a subset $V(\delta) \subset V$ as $V(\delta) := \{v \in V \mid \exists e \in E, e \ni v, \delta \cap e \neq \emptyset\}$ and a coloring map $\mathcal{L}_\delta : V(\delta) \to \{0,1\}$ step by step, as follows. First, pick some edge $e \in E$ that is crossed by δ. Denote its extremities w_0 and b_0, in any arbitrary order. Add $w_0 \in \mathcal{L}_\delta^{-1}(0), b_0 \in \mathcal{L}_\delta^{-1}(1)$. To pass from step j to the step $j+1$, we add $b_{j+1} \in \mathcal{L}_\delta^{-1}(1), w_{j+1} \in \mathcal{L}_\delta^{-1}(0)$ in such a way that the following conditions hold: either $b_j = b_{j+1}$ or $w_j = w_{j+1}$; $b_j b_{j+1} \cap \delta = w_j w_{j+1} \cap \delta = \emptyset$; $b_j w_{j+1} \cap \delta \neq \emptyset$, $w_j b_{j+1} \cap \delta \neq \emptyset$. Here some of the edges here may be empty (degenerate into vertices). It may also happen for some $k < j-1$ that $b_j = b_k, k < j-1$.

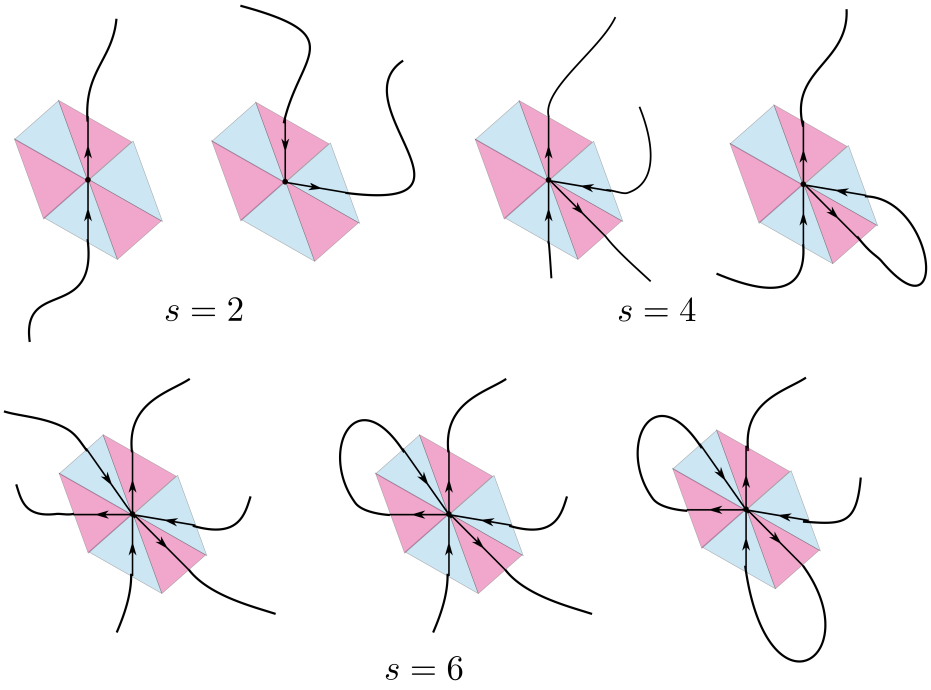

FIGURE 20. Possible behaviors of unbounded flowers in parallel triangle tiling billiard foliations.

Define a subgraph G_k^δ of Λ (for $\Lambda = \Lambda_\Delta$ or $Lambda_\square$), $k = 0, 1$ as a graph with the set of vertices coinciding with $\mathcal{L}_\delta^{-1}(k)$ and two vertices are connected by an edge of Λ, if such an edge exists.

***Theorem 13* (Density property).** — *For any nonsingular triangle tiling billiard trajectory δ, at least one of the graphs G_k^δ is a tree (say, G_0^δ). A trajectory is periodic if and only if G_1^δ has a unique cycle in it. A trajectory δ is not periodic if and only if both of the graphs G_0^δ and G_1^δ are trees.*

The proof of the Density property follows the same strategy as the proof of Theorem 3, we give here a sketch of its proof. Consider the parallel foliation $\mathcal{P}^\delta$ and perturb δ in it onto singular trajectories.

If δ is periodic, the two singular trajectories γ_+, γ_- approaching δ are well defined since there are no accumulating trajectories in the neighbourhood of δ. One of them (say, γ_-) is a bounded flower inside Ω^δ, and another one is a petal of a bigger (not necessarily bounded) flower. In this case, the statement of the Density conjecture follows directly from Theorem 3, since the graph G_1^δ is uniquely defined by G_0^δ as the set of vertices at distance 1 from G_0^δ.

If δ is exceptional then the Density property follows from Theorem 11, δ is an only non-bounded leaf in $\mathcal{P}^\delta$. In this case, each of the graphs G_0^δ and G_1^δ is a spanning tree of the initial graph Λ_Δ. Finally, in order to finalize the proof for a linearly escaping trajectory δ, one classifies possible topological behaviours of unbounded flowers. The Proposition below finishes the proof.

Proposition 12. — *Consider an unbounded flower γ in $v \in V$ with s separatrix segments in Θ_v. Suppose that at least one of these segments defines an escaping ray. Then, up to change of orientation, γ has one of the types listed on Figure 20.*

Proof. — By Proposition 1, it is left to exclude the following two obstructions for the behaviour of some unbounded flower γ. First, if $s = 4$ and there exists a closed petal in γ passing by two opposite triangles. And second, if $s = 6$ and there exist two unbounded separatrix rays passing by neighbouring triangles, and the two bounded petals of the flower have different orientations.

Both of these cases are excluded by a common symmetry argument. In both of the obstructions above, there exists a tile $\theta_0, \theta_0 \ni v$ such that $\gamma \cap \theta_0$ defines an unbounded separatrix ray and θ_0^v is contained inside some petal of γ. Following Proposition 4, one considers a symmetric flower γ^v in the ray foliation. Then γ and γ^v necessarily intersect outside v which gives a contradiction. □

Conjecture 2. — *Density property holds for quadrilateral tiling billiards.*

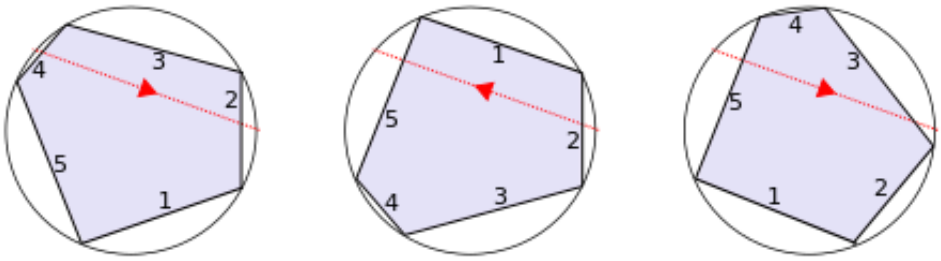

FIGURE 21. *Two iterations of a system of reflections of a pentagon in its circumcircle.* After each iteration, the direction of the chord defined by the parameter τ changes to its opposite. The symbolic code of the orbit $(X, F(X), F^2(X))$ in this case is $w = a_4a_2 \;\; a_2a_5$ for some $F \in \mathrm{CET}^5_\tau$.

This Conjecture is a stronger form of Conjecture 1, it can also be reformulated in terms of scissor cuts. Indeed, we fold a cyclic quadrilateral tiling of the plane into a bellow. Then, we cut along some line in the bellow. Then, the plane "falls into" an infinite number of connected components. The Density property is equivalent to the fact that none of these components contains a full tile.

Does the Density property (and hence, the Tree Conjecture) have a simpler proof based on this interpretation? Of course, a difficulty in proving this property is that when one makes a cut of the bellow, one does not cut out one trajectory but an infinite number of them. Moreover, the Density property doesn't follow purely from folding since there exist locally foldable tilings on which the Tree Conjecture is false.

The next statement follows obviously from Theorem 3 but we present its proof in relation to the reformulation of the Density property we just gave.

Proposition 13. — *There is no triangle tiling billiard trajectory δ that crosses the tiles $\theta^e, e = a, b, c$ and doesn't cross the tile θ, surrounded by them.*

Proof. — Take any trajectory δ, and consider its folding into a chord l in the disk $\mathcal{D}$. We color each vertex $v \in V$ of the plane in one of the two colors depending on what side the vertex $\mathcal{F}(v)$ is with respect to the oriented chord l. Suppose now that δ as in the assumption exists. Then all of the vertices of θ are colored in the same color. Although, the vertices A', B', C' of the tiles θ^e with $e = a, b, c$ that do not belong to θ are all colored in the opposite color. This is impossible since at least one of these three vertices lies on the same side of the chord l as A, B and C, by folding. □

10.3. Symbolic dynamics of maps in CET^n_τ. — Even though there exists no periodic tiling by n-gones with $n \geq 5$, a geometric interpretation of the dynamics of maps in CET^n_τ exists and was already discussed in **[25]**.

Consider some cyclic polygon P with n sides and take $\tau \in \mathbb{S}^1$. This data defines a map F of **reflections in the circumcircle** as follows. Consider a chord in the disk bounded by the unit circle and connecting 0 to τ. Denote the sides of $\mathcal{P}$ by reading the boundary in a counterclockwise order, by $a_1, a_2, \ldots, a_n$. We put $a_{n+1} := a_1$. For any $X \in \mathbb{S}^1$ we inscribe the polygon $\mathcal{P}$ in its circumcircle in such a way that for a vertex $A = a_1 \cap a_n$, one has $A = X$. The map F then sends a polygon into a congruent polygon of different orientation sharing one side with P, by a flip. A label of the side is defined by a positive intersection of $\mathcal{P}$ with a chord defined by τ, see Figure 21. For any n, the data (P, τ) defines a map $F \in \mathrm{CET}^n_\tau$.

The following definition is inspired by our discussion with Pierre Dehornoy.

Take $\mathcal{A}^2_n := \{a_ia_j \mid i, j = 1, \ldots n, i \neq j\}$ an alphabet. Then the map $\mathrm{wd} : \mathcal{A}^2_n \to \{0, 1, -1\}$ defined on the letters by $\mathrm{wd}(a_ia_j) = 1$ if $j = i + 1$, $\mathrm{wd}(a_ia_j) = -1$ if $i = j + 1$, and $\mathrm{wd}(a_ia_j) = 0$ otherwise is the **winding** map. It extends to $\mathcal{A}^2_n$ by additivity. Of course, the winding map is a generalization of the sign map defined in paragraph 5.3.

For the following, we only consider the **periodic trajectories** in the system of reflections in the circumcircle as those that are stable under a small perturbation of the polygon $\mathcal{P}$. We give such a definition since the the drift-periodic trajectories of tiling billiards in triangle and quadrilateral tilings also correspond to periodic trajectories of the system of reflections. One defines a **winding of a periodic trajectory** of the system of reflections in the circumcircle as the winding of its symbolic code.

Example. — A winding for a tour of a vertex in a triangle (quadrilateral) tiling is ± 6 (or ± 4).

Lemma 6. — *A winding of a simple closed curve $\delta, \delta \cap V = \emptyset$ in the triangle (quadrilateral) tiling is equal to ± 6 (± 4) depending on its orientation. Moreover, for any $n \in \mathbf{N}, n \geq 3$, the winding of a periodic trajectory in*

a system of reflections in the circumcircle for a n-polygon is well-defined and equal to $\pm 2n$ if n is odd, and to $\pm n$ if n is even.

Proof. — Consider a vector $v_\delta^\perp$ orthogonal to the curve δ and count the (algebraic) number of turns this vector makes when it moves along δ. One can easily see that this number is exactly $\frac{1}{6}\mathrm{wd}(\delta)$ for the triangle tiling billiard and $\frac{1}{4}\mathrm{wd}(\delta)$ for cyclic quadrilateral tiling billiard by decomposing δ into a sum of loops. Then, we first observe that the winding of a periodic trajectory is well-defined, i.e. doesn't depend on the string representation of the periodic trajectory. Second, the only change in winding is done by the words that use subsequent letters. Even though for $n > 4$ the corresponding tiling doesn't exist, one still can unfold the trajectory to some broken trajectory in a tiling with self-coverings. When one comes back to the same tile in the system of reflections, one comes back to the same tile on such an unfolding. □

***Conjecture 3* (Winding Conjecture).** — *For any map $F \in \mathrm{CET}_\tau^n$, a winding number is an invariant, i.e. the same for all of its periodic trajectories .*

The Winding Conjecture is our attempt to generalize the Tree Conjecture for any family CET_τ^n, for all $n \geq 3$. From Theorems 3 and 13 it follows, that the Winding Conjecture holds $n = 3$. We believe that the Winding Conjecture holds for at least $n = 4$ and concerns the asymptotic cycle for families of translation surfaces. The difficulty is that these families are not generic, so classical results do not apply.

Problem. Give an explicit description of minimal maps in CET_τ^n for any $n \geq 3$.

This Problem is answered for $n = 3$ in Theorem 10. Already for $n = 4$ this question is open. In [**25**] it has been shown that for $n = 3$ and $n = 4$ minimal maps in CET_τ^n belong to the hyperplane $\tau = \frac{1}{2}$. Can provide a homological argument to prove this statement? Moreover, we find interesting to study the set of length parameters of minimal maps in CET_τ^4 inside the hyperplane $\{\tau = \frac{1}{2}\}$, a next-dimension analogue of the Rauzy gasket. Is it Lebesgue measure 0 and what is its Hausdorff dimension?

For $n \geq 5$ one may exhibit the examples of minimal maps in CET_τ^n outside the hyperplane $\{\tau = 1/2\}$. One could speculate that such a behavior of the family CET_τ^n (minimality implying $\tau = \frac{1}{2}$ for $n = 3, 4$ but only for these n) is related to the famous Novikov's conjecture on the chaotic sections of genus 3 subsurfaces of a 3-torus. Indeed, the squares of the maps in CET_τ^n for $n = 3, 4$ are interval exchange transformations corresponding to genus 3 flat surfaces.

APPENDIX. ON *TRIANGLE TILING BILLIARDS AND THE EXCEPTIONAL FAMILY OF THEIR ESCAPING TRAJECTORIES: CIRCUMCENTERS AND THE RAUZY GASKET*

While working on this article we have found a mistake in one of the proofs in our previous work with P. Hubert. This mistake does not influence the principal results of [**25**], except for the proof of $4n + 2$ Conjecture. The present work gives a new set of tools for the study of triangle tiling billiards, and reproves all of the results in [**25**], in a simpler way.

Here we revisit the proof of the key proposition in the proof of the $2n + 2$ Conjecture in [**25**]. We remind the statement as well as the idea of the initial proof, and then point out the hole. We remind our reader that the work [**25**] approached the maps in the family CET_τ^3 with a tool of a standard Rauzy-Nogueira induction.

Proposition 14. — [**25**] *Take $F = F_\tau^{l_1,l_2,l_3} \in \mathrm{CET}_\tau^3$ such that $\frac{l_i}{l_j} \notin \mathbf{Q}$ for any $i \neq j$. Suppose that the Rauzy-Nogueira induction stops for F at some 4-interval exchange transformation F'. Then for any interval $Y \subset I$ of continuity for F' such that $F'(Y) = Y$, the restriction $F'|_Y$ is an involution.*

A strategy proof in [**25**] is straightforward, take a map F' with $F'|_Y = \mathrm{id}$, follow backwards the induction and prove that it never ends in CET_τ^3. The argument is correct except for the case when $F' = \begin{pmatrix} Y & * & * & \bar{X} \\ Y & * & * & \bar{X} \end{pmatrix}$. We argue that the back-ward path has to go up into Y losing to some (flipped) Z, as in

$$\begin{pmatrix} Y & * & * & \bar{X} \\ Y & * & * & \bar{X} \end{pmatrix} \leftarrow \begin{pmatrix} \bar{Y} & \dots & \bar{Z} \\ \bar{Z} & \dots & \bar{Y} \end{pmatrix}. \tag{24}$$

Then one concludes $Z = X$. A mistake in this reasoning is that for a matrix represented by the right-hand side of (24) its number of columns may potentially be smaller than 4, i.e. Z is not necessarily equal to X. Indeed, there exist an open set of fully flipped 4-IET for which $Z \neq X$, for example the Rauzy induction can stop for them, and then reiterated on a smaller interval as in

$$(25)\qquad \begin{pmatrix} \bar{Z} & \bar{W} & \bar{X} & \bar{Y} \\ \bar{Y} & \bar{Z} & \bar{W} & \bar{X} \end{pmatrix} \xrightarrow{X>Y} \begin{pmatrix} \bar{Z} & \bar{W} & Y & \bar{X} \\ Y & \bar{Z} & \bar{W} & \bar{X} \end{pmatrix} \xrightarrow{W>Y} \begin{pmatrix} \bar{Z} & \bar{Y} & \bar{W} & \bar{X} \\ \bar{Y} & \bar{Z} & \bar{W} & \bar{X} \end{pmatrix} \xrightarrow{Z>Y} \begin{pmatrix} Y & \bar{Z} & \bar{W} & \bar{X} \\ Y & \bar{Z} & \bar{W} & \bar{X} \end{pmatrix}.$$

One can finish the proof along the lines of [**25**] but the proof becomes a case-by-case study of a big graph. Moreover, a chain given in (25) can be modified in order to construct a counterexample to Proposition 14 for the maps in the family CET^4_τ. Indeed, it suffices to add a fifth column $\begin{pmatrix} \bar{V} \\ \bar{V} \end{pmatrix}$ to every matrix in a chain. Then, a matrix $\begin{pmatrix} \bar{Z} & \bar{W} & \bar{X} & \bar{Y} & \bar{V} \\ \bar{Y} & \bar{Z} & \bar{W} & \bar{X} & \bar{V} \end{pmatrix}$ corresponds to the dynamics of a map in CET^4_τ. It suffices to define $I_1 := Z, I_2 := W, I_3 := X, I_4 := Y \cap V$. This illustrates how the orbits of periods different from $4n+2$ may appear in cyclic quadrilateral tiling billiards, see paragraph 10.1. Moreover, the proof of the integrability result for CET^4_τ (Proposition 9 in [**25**]) is hence not finished.

To conclude, all of the statements of [**25**] for triangle tiling billiards are correct, even though the proof of the $4n+2$ Conjecture is not finished. Moreover, this work doesn't provide any understanding on the dynamics of quadrilateral tilings since the [point 2, of Theorem 7] is false, and the proof of the [Proposition 9] is not finished. We strongly believe that the integrability property holds for almost all quadrilateral tiling billiards, and reflects an interesting subcase of Novikov's conjecture, see discussion at the end of Section 10. It can be checked explicitely by the study of big Rauzy-Nogueira graphs but we hope to find a simpler proof in the future.

ACKNOWLEDGEMENTS

I am grateful to Pierre Arnoux, Dmitry Chelkak, Charles Fougeron, Pascal Hubert, Victor Kleptsyn, Paul Mercat, Julien Lavauzelle, Pierre Dehornoy, Valente Ramirez, Ferrán Valdez and Barak Weiss for interesting discussions. All of the figures representing triangle tiling billiard trajectories are drawn using the program by P. Hooper and A. St Laurent accessible online, see `http://awstlaur.github.io/negsnel/`. The research for this paper has been done in many places and many countries (anyway, trees are everywhere...). I am especially thankful to IRMAR at University of Rennes 1, as well as to CIRM in Marseille where I have fallen in love with the Tree Conjecture presented in a talk [**17**] by Diana Davis, on the 14th February 2017.

References

[1] Online encyclopedia of integer sequences, `https://oeis.org/A0000213`

[2] N. C. Affolter, *Miquel Dynamics, Clifford Lattices and the Dimer Model*, preprint (2018)

[3] P. Arnoux, J. Bernat, X. Bressaud, *Geometrical models for substitutions*, Exp. Math. 20, 97–127 (2011)

[4] P. Arnoux, *Un exemple de semi-conjugaison entre un échange d'intervalles et une translation sur le tore*, Bull. Soc. Math. France 116, 489–500 (1988)

[5] P. Arnoux, *Un invariant pour les échanges d'intervalles et les flots sur les surfaces*, doctoral thesis (1981)

[6] P.Arnoux, G. Rauzy, *Représentation géométrique des suites de complexité* $2n+1$, Bulletin de la SMF., 119:2, 199–215 (1991)

[7] P.Arnoux, S. Starosta, *The Rauzy gasket*, Birkhäuser Boston. Further Developments in Fractals and Related Fields, Springer Science+Business Media New York, 1–23, Trends in Mathematics (2013)

[8] P. Arnoux and J.C. Yoccoz, Construction de difféomorphismes pseudo-Anosov, C. R. Acad. Sci. Paris 292:1, no. 1, 75–78 (1981)

[9] A. Avila, V. Delecroix *Some monoids of Pisot matrices*

[10] A. Avila, P. Hubert, A. Skripchenko, *Diffusion for chaotic plane sections of 3-periodic surfaces*, Inventiones mathematicae, 206:1, 109–146 (2016)

[11] A.Avila, P. Hubert, A. Skripchenko, *On the Hausdorff dimension of the Rauzy gasket*, Bulletin de la société mathématique de France, 144:3, 539–568 (2016)

[12] P.Baird-Smith, D.Davis, E.Fromm, S.Iyer, *Tiling billiards on triangle tilings, and interval exchange transformations*, preprint, `http://www.swarthmore.edu/NatSci/ddavis3/triangle_tiling_billiards.pdf` (2018+)

[13] V. Berthé, J. Cassaigne, W. Steiner *Balance properties of Anoux-Rauzy words*

[14] D. Chelkak, B. Laslier, M. Russkikh *Dimer model and holomorphic functions on T-embeddings of planar graphs*, preprint (2019+)

[15] T. Coulbois, M. Minervino *Tree substitutions and Rauzy fractals*, preprint, `https://arxiv.org/abs/1711.03535` (2017)

[16] D. Davis, W. Patrick Hooper, *Periodicity and ergodicity in the trihexagonal tiling*, accepted pending revision in Commentarii Mathematici Helvetici (2018)

[17] D. Davis, *Interval exchange transformations from tiling billiards*, talk at the conference Teichmüller Space, Polygonal Billiard, Interval Exchanges in CIRM, Marseille, `https://www.youtube.com/watch?v=CO5bVlRWmow&t=2175s` (2017)

[18] D. Davis, K. DiPietro, J. Rustad, A. St Laurent, *Negative refraction and tiling billiards, to appear in Advances in Geometry* (2016)

[19] R. De Leo, I. Dynnikov, *Geometry of plane sections of the infinite regular skew polyhedron* $\{4, 6 \mid 4\}$, Geom. Dedicata 138, 51–67 (2009)

[20] P. Glendinning, *Geometry of refractions and reflections through a biperiodic medium*, Siam J. Appl. Math., Society for Industrial and Applied Mathematics 76:4, 1219–1238 (2016)

[21] S. Guenneau, S. Anantha Ramakrishna, Amar C. Vutha, J.B. Pendry *Negative refraction in 2-D checkerboards related by mirror anti-symmetry and 3-D corner lenses*

[22] S. Guenneau, B. Gralak, J.B. Pendry *Perfect corner reflector*, Optics letters, 30:10 (2005)

[23] P. Hooper, Alexander St Laurent, *Negative Snell law tiling billiards trajectory simulations*, `http://awstlaur.github.io/negsnel/`

[24] W. Patrick Hooper, B. Weiss, *Rel leaves of the Arnoux-Yoccoz surfaces*, Selecta Mathematica, 24:2, 875–934 (2018)

[25] P. Hubert, O. Paris-Romaskevich *Triangle tiling billiards and the exceptional family of their escaping trajectories: circumcenters and Rauzy gasket*, Experimental mathematics, `https://doi.org/10.1080/10586458.2019.1583615` (2019)

[26] T. C. Hull *The combinatorics of flat folds: a survey*, Origami: Third International Meeting of Origami Science, Mathematics and Education, T. Hull editor A K Peters, Natick, MA, 29–38 (2002)

[27] M. Keane, *Interval exchange transformations* Math. Z. 141, 25-31 (1975)

[28] R. Kenyon, W. Y. Lam, S. Ramassamy, M. Russkikh *Dimers and circle patterns* (2019)

[29] J. H. Lowenstein, G. Poggiaspalla, and F. Vivaldi, *Interval exchange transformations over algebraic number fields: the cubic Arnoux-Yoccoz model*, Dynamical Systems, 22(1), 73–106 (2007)

[30] Y. Liu, S. Guenneau, B. Gralak, S. A. Ramakrishna *Focusing light in a bianisotropic slab with negatively refracting materials*, J. Phys.: Condens. Matter (2013)

[31] A. Mascarenhas, B. Fluegel *Antisymmetry and the breakdown of Bloch's theorem for light*, unpublished draft

[32] C. McMullen, *Cascades in the dynamics of measured foliations*, 48:1, Annales Scientifiques de l'École Normale Supérieure (2015)

[33] C. McMullen, *Navigating moduli space with complex twists*, J. Eur. Math. Soc. (JEMS) 15, 1223–1243 (2013)

[34] A. Nogueira, *Almost all interval exchange transformations with flips are nonergodic*, Ergodic Theory Dynam. Systems 9:3, 515-525 (1989)

[35] G. Rauzy, Nombres algébriques et substitutions, Bulletin de la Société Mathématique de France 110, 147-178 (1982)

[36] A. Ramakrishna, S. Guenneau, S. Enoch, G. Tayeb, B. Gralak *Confining light with negative refraction in checkerboard metamaterials and photonic crystals*, Physical review, 25 (2007)

[37] G. Rauzy, *Échanges d'intervalles et transformations induites*, Acta Arith., 34(4):315–328, (1979)

[38] A. Skripchenko, S. Troubetzkoy, *On the Hausdorff dimension of minimal interval exchange transformations with flips*, Journal London Mathematical Society, to appear.

[39] M. Schmoll, *Spaces of elliptic differentials*, in Algebraic and topological dynamics, S. Kolyada, Yu. I. Manin and T. Ward eds., Cont. Math. 385, 303–320 (2005)

[40] A. Zorich, *Flat surfaces*, in Frontiers in number theory, physics and geometry, P. Cartier, B. Julia, P. Moussa and P. Vanhove (eds), Springer (2006).

[41] B. Wood *Metamaterials and invisibility*, C. R. Physique 10 (2009)

Olga Paris-Romaskevich • *E-mail :* <olga@pa-ro.net> • *Url :* <http://olga.pa-ro.net/>